DOI: 10.1002/ ((please add manuscript number))
Article type: Full Paper

Tailor-made molecularly imprinted polymer for selective recognition of the urinary tumor marker pseudouridine

Aleksandra Krstulja, Stefania Lettieri, Andrew J. Hall,*, Vincent Roy, Patrick Favetta and Luigi A. Agrofoglio*

Dr. A. Krstulja, Dr. V. Roy, Dr. P. Favetta, Pr. L.A. Agrofoglio
ICOA UMR CNRS 7311, Univ. Orléans,
Rue de Chartres 45067 Orléans, France
E-mail: luigi.agrofoglio@univ-orleans.fr

Dr. S. Lettieri, Dr. A.J. Hall
A Medway School of Pharmacy- Univ. Greenwich & Kent
Chatham, Kent, ME4 4TB, UK
E-mail: a.hall@kent.ac.uk

Keywords: pseudouridine, tailor-made monomer, molecular recognition, imprinted polymer, cancer

Abstract: Pseudouridine (Ψ) is an important urinary cancer biomarker, especially in human colorectal cancer (CRC). Disclosed herein is the first pseudouridine molecularly imprinted polymer (Ψ-MIP) material obtained from tailor-engineered functional monomers. The resulting MIP imprint exhibits a remarkable imprinting factor greater than 70. It is successfully used for the selective recognition of pseudouridine in spiked human urine. This selective functionalized material opens the route to the development of inexpensive disposable chemosensors for non-invasive CRC diagnosis and prognosis.

1. Introduction

Pseudouridine (5-β-D-ribofuranosyluracil) (Ψ) is a C-glycoside type of naturally modified nucleoside, found in rRNA and tRNA of bacterial and mammalian origin.[1] In the growth of cancer cells or some viral disease, due to the high turnover of tRNA, concentrations of

pseudouridine have been released in biofluids, allowing to begin a highly relevant molecule for monitoring of cancer growth.[2] Since Ψ does not undergo regular metabolic degradation processes because of the lack of the enzyme that can metabolize C-glycoside nucleosides,[3] it found in the human urine. The difficulty is to select an appropriate method to monitor selectively this biomarker among several dozens of nucleoside analogues [4]. The common techniques for its detection, enzyme-linked immunosorbent assay (ELISA),[5] micellar electrokinetic capillary chromatography (MECC),[6] matrix assisted laser desorption ionization-time of flight mass spectrometry (MALDI-TOF MS)[7] require costly and time-consuming equipment and often involve preliminary treatments with a risk to lose or modify the active compound. So, to meet this kind of challenge, recently, biosensors based on well-known molecularly-imprinted polymers (MIP)[8-11] have gained of interest since they are compatible with different transducers and can recognize a molecule without pre-analytical preparations. However, the cornerstone of such polymer-based receptors remains the design of their material component, which defines their specificity and overall quality. For pseudouridine, a C-C glycosidic isomer of uridine (U), which shares with U similar physico-chemical data, the conception of highly selective MIP is very challenging (**Figure 1**). The technique of molecular imprinting aims to replicate synthetically the phenomenon of molecular recognition occurring in biological systems, such as enzymes or antibodies.[12] It provides synthetic materials possessing selective cavities (size, shape and functionality) of a given molecule, called guest molecule or template molecule, here pseudouridine. According to the manner how the template is connected to the functional monomer and subsequently to the selective binding sites, the molecularly imprinted polymer (MIP) can show a such selectivity that this material is sometimes named “plastic antibody”.[13] To obtain this high molecular recognition ability, the monomer which functionalizes the material is the key point of the formulation. We have chosen to synthesize selective monomers able to interact with

Ψ through multiple hydrogen bonds, to form a 1:1 pre-polymerization complex, in order to enhance its adsorption on imprinted polymer in comparison to a non-imprinted one. This type of approach is known as stoichiometric non-covalent interactions imprinting, as described by Tanabe et al.[14] The major advantages of this non-covalent imprinting is to work without excess of small functional monomers, such as acrylamide, acrylic acid,... in order to move the equilibrium to the formation of the pre-polymerization complex[15] and to decrease non-specific interactions. So, in this study, we developed the first pseudouridine-MIP obtained from tailor-engineered functional monomers, able to discriminate, with remarkable imprinting factors and selectivities, Ψ from close nucleoside analogues such as U, in spiked human urine.

[FIGURE 1]

2. Results and Discussion

2.1. Design of imprinted materials

We used a stoichiometric non-covalent imprinting approach, in order to reduce the number of non-specific interactions present in the obtained MIPs and to show fast binding kinetics, contrary to classical non-covalent and covalent approaches, respectively.[16,17] An aprotic porogenic solvent and a derivative of Ψ were used to promote strong non-covalent associations, by hydrogen bonding interactions, between the nucleobase part of Ψ and tested monomers, ensuring selectivity of recognition when close nucleoside analogues were present in the sample. Thus, the 2',3',5'-tri-O-acetyl pseudouridine (TAcΨ) was used as a dummy template instead of Ψ to overcome the poor solubility of the latter in organic aprotic solvents, generally preferred for the imprinting process.[18] A set of four monomers which differed in

the number of theoretical recognition sites and thermodynamic preferences for the complexation with Ψ was tested (**Figure 2**).

[FIGURE 2]

2.1.1. Choice of functional monomers

Acrylamide (**1**) was chosen as a reference to classical non-covalent imprinting and should interact with the C(=O)NH groups present on pseudouridine, (**Figure 3**).[19,20] The 2,6-bis(acrylamido)pyridine monomer **2** was already used in the stoichiometric imprinting of uracils.[21-23] Monomer **3**, inspired by the polymerizable version of a biotin-cleft,[24] allowed to evaluate selective interactions with the additional –N(1)H of Ψ. Monomer **4**, inspired from barbiturate recognition,[25] was used to create more anchorage points than monomers **2** or **3** by hydrogen bonding. The synthesis of monomers **2**, **3** and **4** are described in supporting informations part.

[FIGURE 3]

2.1.2. Choice of polymerization solvent

Solubility tests of the TAcΨ and monomers (**1-4**) were performed in a range of solvents (chloroform, acetonitrile, dimethyl sulfoxide and 1,4-dioxane/THF (3/1, v/v), differing in their isoelectric constants and hydrogen bonding capabilities. The testing was carried out separately by raising the mass of the templates or monomer in 1 mL of solvent and subsequently mixing until precipitation was observed. The wanted solubility limit for the polymers synthesis was 100 mM, (**Table S1**). Chloroform was the solvent of choice for all

formulations except those containing monomer **4**, for which a binary ether type solvents mixture presenting the same Hansen Solubility Parameters was selected.[26]

2.1.3. Stability of pre-polymerisation complexes

The pre-polymerisation complexes between the functional monomers 1-4 and the TAcΨ was studied by NMR titrations on a 1:1 binding model to obtain the apparent binding constant (K_{app}) and the maximum induced shift Δ_{HG}; the isothermal titration calorimetry (ITC), performed in chloroform, allowed calculating the K_b, N, ΔH and ΔS, meanwhile the interaction Gibbs free energies of complexes were calculated by molecular modelling. All thermodynamic parameters (**Figures S1, S2**) are shown in **Table 1**.

[Table 1]

By observing the association constant in ^{1}H-NMR titration, we believe the strength of association inside each complex can be explained by the number of theoretically "positive" (hydrogen bonding) and "negative" interactions (steric effect) existing between template and monomer (**Figure 3**).[27,28] ^{1}H-NMR titration study confirmed the preference of monomer **3** for a more stable interaction with the Ψ nucleobase where a higher value of K_{app}=352±49 M^{-1} was obtained for complex TAcΨ/**3**. Therefore, the complex stability established by NMR was TAcΨ/**3** > TAcΨ/**2** > TAcΨ/**4**.

To support this finding, for TAcΨ/**3** and TAcΨ/**2** complexes, a computational approach based on DFT calculations of molecular interactions Gibbs free energies (ΔG), for the 1:1 complexes in $CHCl_3$, as well as in water (anticipating the behavior of the polymer in aqueous medium), confirmed the order of ligand stability as **3** > **2**. Moreover, the ITC titration confirmed 1:1 stoichiometry and indicated, by the negative ΔG values, that formation of

complexes in chloroform was a spontaneous process. The process of complexation was exothermic and driven by hydrogen and van der Waals interactions.[29] Moreover, the difference in ΔH measurements between complexes TAcΨ/**2** and TAcΨ/**3** reflected the differences in the number of favourable interactions existing in each complex.[30] The negative entropy implicated in TAcΨ/**3** formation showed a reduction of degrees of freedom in the system showing better complexation than for complex TAcΨ/**2**.[31]

These complementary techniques showed that the best complexes and affinity of monomers toward TAcΨ are **3 > 2 > 4> 1**.

2.2. Optimized synthesis of imprinted polymers

To explore the influence of those monomers on the polymer recognition behavior, four bulk polymers were prepared from template TAcΨ, monomers **1-4**, ethylene glycol dimethacrylate (EGDMA) as the cross-linker and the polymerization initiator 2,2'-azobis(2,4-dimethylvaleronitrile (ABDV). Along with the imprinted polymers (MIPs-1 to -4), the corresponding non-imprinted polymers (NIPs-1 to -4) were synthetized (**Table 2**).

[TABLE 2]

Obtained MIPs were packed in a stainless-steel HPLC columns in order to determine the selectivity factor (α), imprinting factor (IF), retention factor (k), affinity and capacity of each polymer for thirteen nucleosides: the template (TAcΨ), the target compound (Ψ), some pyrimidine nucleosides (**6**, **7**, **8**, **11**) and seven purine purine nucleosides (**9**, **10**, **12**, **13**, **14**, **15**, **16**) (**Figure 4**).

[FIGURE 4]

2.3. Imprinting efficiency evaluation by HPLC

The retention based on polar non-covalent interactions was characterized in acetonitrile as mobile phase (**Table S2, Figure S3**), and the efficiency of recognition was evaluated in synthetic urine (**Figure S4, Table S3**). The use of monomers with various size, flexibility and interaction points produces polymers that exhibit different recognition behaviours.

As expected, the acrylamide based MIP-1 gave poor retention behaviour compared to NIP in both organic and aqueous phase, meanwhile for MIP-4 a low specificity of this polymer was observed (correlated to the titration results). MIP-2 and MIP-3 showed stronger retention for the template, target and close pyrimidine analogues in organic and aqueous medium. Among all polymers, MIP-3 demonstrated high recognition for target Ψ in synthetic urine, giving a very high IF value of 70 (**Figure S4C**), as predicted by the DFT results in water. In addition, the retention of other modified nucleosides was significantly lower, demonstrating the efficacy of tailored-made monomer **3** for selective recognition of Ψ. This result is exceptional compared to similar previously published studies for the recognition of nucleosides in an aqueous phase.[32]

2.4. Evaluation of the affinity constant and adsorption capacity of polymers

The affinity constant and number of usable binding sites per unit polymer mass were determined for each polymer by frontal chromatography. The tested models used calculations based on isothermal (25°C) equilibrium adsorption thermodynamics. From each concentration step, the corresponding amount of the bound analyte (Q) was calculated and plotted against the corresponding template concentration (Cf) in the organic mobile phase. The experimental results (**Figure 5**) demonstrated that MIP-3 has a much higher capacity than other polymers based on the largest difference between the level of adsorption isotherms compared to NIP-3, and the fact that MIPs-1, 2 and 4 reached a saturation point at a lower level than MIP-3.

Further, in the low concentration range (**Figure 5, insert**), MIP-2 and MIP-3 showed some significant adsorption and possible presence of theoretically high energy binding sites with a mean affinity constant of $K_a > 10^6$ M^{-1}, and with very low non-specific adsorption on the corresponding NIPs. This confirms that MIP-3 has a high recognition capacity for target Ψ.

[FIGURE 5]

Concerning the modeling of adsorption isotherms (**Table S5**), MIP-2 and MIP-3 were fitted better to a bi-Langmuir model, describing a more homogeneous surface with theoretically only two types of binding sites (high and low affinity). However, MIP-2 did not show a great difference in affinity between the low and high affinity sites. Furthermore, looking at the overall number of both types of binding sites, MIP-3 had a higher number of binding sites, with the highest affinities among all the polymers, with 3.7 μmol.g^{-1} of high affinity (K_a=9.5x10^3 L.mol^{-1}) vs. 43 μmol g^{-1} of low affinity (K_a=0.63x10^3 L.mol^{-1}) binding sites. This result is in agreement with the high performance liquid chromatography (HPLC) retention data discussed previously. MIP-4 was the only polymer that showed the best fit to the Langmuir-Freundlich model, describing both saturation and sub-saturation areas, giving a total number of binding sites of 4.8 μmol.g^{-1} with an affinity of K_a=0.64x10^3 L.mol^{-1} and confirming that MIP-4 has at least some binding capability, as demonstrated in the HPLC study; however, it has a low specificity as demonstrated by the small difference between MIP and NIP adsorption capacity levels (**Figure 5**). For NIP-1, -2, and -4, adsorption of template fitted a Langmuir-Freundlich model, and for NIP-3 to the Freundlich model. From the results of these fits, though not all the same, we conclude that all four NIPs exhibit a homogenous nature of adsorption ($m \geq 0.70$).[33]

2.4. Selective extraction of pseudouridine from synthetic urine

MIP-3 was the best candidate for selective recognition of Ψ in real human biological sample and it was used as a molecularly imprinted solid phase extraction (MISPE) sorbent. At first, synthetic urine was used in order to mimic the real sample and to observe the influence of the complex matrix on polymer recognition capabilities.[34] The cross-rebinding studies were performed using a mixture of Ψ and its close analogues **5**, **6** and **7** (**Figure 4**), which can be found in the urine of colorectal cancer (CRC) patients. 5-Fluorouracil (**5**), which lacks the same chemical functionalities to interact with the polymer[35] was included since it is a pyrimidine analogue frequently used as a cytostatic in cancer treatment.

With the optimized extraction protocol, the Ψ recoveries were up to 95% and ca. 5% on MIP-3 and NIP-3, respectively (**Figure S6**). Then, the MISPE procedure was tested with a real urine sample, (**Figure 6**).

[FIGURE 6]

Urine, spiked with 5 µg.mL^{-1} of the 4 standard nucleosides given previously (Ψ, **5**, **6** and **7**), was extracted on both MIP-3 and NIP-3 and analysed with a validated HPLC-UV method (Table S10). The recovery for MIP-3 (92±2%) and NIP-3 (2±2%), respectively, shows a very clean extract and the possibility for MIP-3 to recognize and capture very selectively Ψ in biological fluids. The MISPE method was repeated three times on the same cartridge with the RSD < 20% at the recovery step (**Table S7**).

3. Conclusion

In conclusion, we have reported for the first time a water-compatible imprinted polymer obtained by a stoichiometric approach with a tailor-made functional monomer, for selective recognition of pseudouridine urinary tumor marker, with an IF of 70. Indeed, in the conception phase, high energy complex between pseudouridine and monomer **3** was confirmed both by the ^{1}H-NMR and ITC host-guest studies. Furthermore, in the HPLC

evaluation as stationary phases, among the four synthesized polymers, those using complementary 2,6-diamino pyridine and isopthaloyl derivatives, as monomers **2** and **3**, exhibited the best behaviour with higher retention times and very good selectivity for the Ψ in both organic and aqueous media. The binding affinity isotherms constructed using frontal analysis method best fitted to a Bi-Langmuir adsorption model for both MIP-2 and MIP-3, with $K_a \geq 10^3$. In term of capacity, MIP-3 showed higher total number of binding sites with elevated binding capacity compared to the other polymers. In addition, the results of textural properties analysed using of MIPs, confirmed a mesoporous structure of the polymers, and have shown that significant difference in the surface morphology, was obtained for MIP-3 in respect to its corresponding NIP-3. While the results for textural properties of other prepared MIPs are quite similar when compared to their NIPs. These results further demonstrate that the stability of complex TAcΨ/**3** during polymerization was important in yielding defined and easily accessible surface cavities, and can explain better binding capacity of MIP-3 obtained in frontal analysis. Therefore, owing to its good properties in both chromatographic and morphological properties, MIP-3 was evaluated for the application by the MISPE studies. We have successfully developed a MISPE procedure for the use of the synthesised polymer in extraction of pseudouridine from aqueous media. Application in synthetic urine was compared with that of real urine sample, where high extraction capabilities (95%) of the MIP-3, specificity ($IF_{recovery} > 40$) and selectivity in the cross-rebinding studies were demonstrated. This Ψ-MIP, thanks to its very high selectivity, its ease of polymeric synthesis, its use in an aqueous medium, opens the route to the development of MIP-based chemosensors[36], based on differential pulse voltammetry, capacitive impedimetry or piezoelectrical microgravimetry response,[10] as promising new tools for cancer biomarker determination.

4. Experimental Section

Materials: All solvents and reagents were purchased from Sigma–Aldrich (Saint-Quentin Fallavier, France) and used as received. Pseudouridine (Ψ, 98%) was obtained from Carbosynth (Compton, UK). 2',3',4'-tri-O-acetylpseudouridine (TAcΨ) was prepared from pseudouridine and acid anhydride using a literature method (cf. supporting informations).[37] The nucleosides (see **Figure 4**) 5-fluorouracil (**5**), cytidine (**8**), guanosine (**9**), adenosine (**10**), N^4-acetylcytidine (**11**), 8-hydroxy-2'-deoxyguanosine (**12**), 1-methylinosine (**13**), 1-

methylguanosine (**14**), 7-methylguanosine (**15**) and 1-methyladenosine (**16**) were purchased from Sigma–Aldrich (Saint-Quentin Fallavier, France). Uridine (**6**) and 5-methyluridine (**7**) were purchased from Alfa Aesar (Schiltigheim, France). All the nucleoside bases, nucleosides and their analogues were stored at 4°C and used as received. Azo-bis-dimethylvaleronitrile (ABDV) (DuPont, Netherlands) was kept at -20°C. Acrylamide (**1**) was purchased from Sigma-Aldrich (Dorset, UK), and monomers (**2**), and (**3**) plus (**4**) were synthesised following the protocol established by K. Yano et al. [38] or as described below, respectively. Ethylene glycol dimethacrylate (EGDMA) was purchased from Sigma–Aldrich (Saint-Quentin Fallavier, France) and purified by distillation before use. Deionised water (~18 mΩ) used for the analysis and preparation of solutions was obtained using a water purification system (Millipore, Fontenay-sous-Bois, France). Surface area analyses were performed at 77K by Brunauer–Emmett–Teller (BET) on an ASAP 2020 surface area and porosity analyser (Micromeritics Instrument Corporation, Creil, France). The studies were made using 60 mg of each polymer, which was degassed overnight at 100°C to remove adsorbed gases and moisture. The ^{1}H-NMR and ^{13}C-NMR spectra were obtained on a JEOL ECA, 400MHz FT NMR Spectrometer (Jeol, UK). Chemical shifts are reported in ppm on the δ scale relative to TMS as internal standard or to the solvent signal used. HRMS spectra were obtained using a Waters Synapt G2 TOF mass spectrometer (Waters, Elstree, UK) with an electrospray ionization probe in positive mode. HPLC analyses were performed using an Agilent Infinity 1260 system equipped with a diode array detector and a binary pump (Agilent, Les Ulis, France). The HPLC analyses of extraction samples, and validation of the used HPLC analysis method, was performed using a PGC Thermo Hypercarb® (ThermoFisher Scientific, Courtaboeuf, France) column (150 × 2.1 mm i.d., 5 μm) with UV detection at 260 nm for all analytes. For frontal analysis stainless steel chromatographic columns (50 mm x 4.6 mm i.d.) were packed using the SSI “pack in a box” system (Restek, Paris, France).

Solubility tests: of the TAcΨ and monomers (1-4) were performed in a range of solvents differing in their isoelectric constants and hydrogen bonding capabilities. The testing was carried out separately by raising the mass of the templates or monomer in 1 mL of solvent and subsequently mixing until precipitation was observed. The wanted solubility limit for the polymers synthesis was 100 mM. The results are presented in **Table S1**.

Molecular modelling: all the density functional theory (DFT) computations were performed on the Beowulf cluster at the Institute of Pharmacology Polish Academy of Sciences (IPPAS) in Cracow (Poland). The B3LYP (Becke-Style 3-Parameter DFT using the Lee–Yang– Parr correlation function) with 6-31+G (d,p) basis set was used for geometry optimization to obtain minimum energy structures. In order to avoid the basis-set superposition error (BSSE) related with intermolecular interactions theory, the counterpoise (CP) correction was applied to complex calculations in order to obtain accurate computation of molecular interactions Gibbs free energies by DFT methods.[39] Interaction Gibbs free energies of complexes were calculated using Eq. S1, where ΔG is the change in Gibbs free energy on the formation of template–monomer complex, $G_{template–monomer}$ complex is the Gibbs free energy of template–monomer complex, $G_{template}$ is the Gibbs free energy of template and $G_{monomer}$ is the Gibbs free energy of monomer molecules. All calculations were performed in Jaguar [40,41] and shown in **Table 1**.

Equation 1: $$\Delta G = G_{template–monomer\ complex} - [G_{template} + G_{monomer}]$$

NMR titrations: The complexation induced shift (CIS) of a relevant proton between the functional monomers (1 to 4) and 2',3',4'-Tri-O-acetylpseudouridine (TAcΨ) was analysed in deuterated chloroform. To a 1 mM monomer solution an increasing volume of template 10 mM stock solution was added as a guest molecule (G). The shift (Δδ) of the protons in the monomer amido functionalities were followed (NMR titration spectra are shown in **Figure S1** and **Table 1**). The Δδ was plotted against the concentration of free guest and the curve that is produced is fitted to a non-linear binding isotherm, using OriginPro 8.5.1. The apparent binding constant (K_{app}) and the maximum induced shift Δ_{HG} made by the

complex are calculated from the equation of the curve with the help of equation S2, based on a 1:1 binding model.[42]

Equation 2: $$\Delta\delta = \frac{K_{app}.[G]}{1+K_{app}.[G]}\Delta_{HG}$$

ITC titrations: Calorimetric measurements were performed in chloroform on a computer-controlled VP-ITC microcalorimeter (Microcal, GE HealthCare, Aulnay-sous-Bois, France) against a reference solution of 100% chloroform. Binding curves were obtained from nonlinear analysis of the isotherms using Origin 7 (OriginLab Corp.) analysis package provided by Microcal, Inc. The software allowed calculating the K_b, N, ΔH and ΔS.[43] Experiments were carried out in anhydrous chloroform, where the 0.2 mM solution monomer (2 mL) was placed in the calorimeter cell, and the titration syringe was loaded with 2 mM of the template (at a 10 times higher concentration of the guest to the host). Test (blank) titrations were carried out with only solvent in both syringe and the cell to be sure that the device is clean and no background causing errors would appear. The titrations were obtained at 20°C (293.15 K) with 28 injections of 10 µL each, and time intervals of 180s with a reference power of 15 µcal.s^{-1}. All thermodynamic parameters are shown in **Table 1** and curves of titration in **Figure S2.**

Synthesis of polymers: Following the formulations in **Table 2**, for the synthesis of MIPs, the template, monomer and EGDMA in $CHCl_3$ were introduced to a borosilicate polymerization tube, cooled on ice and degassed for 5 min with nitrogen bubbling in order to remove dissolved oxygen. ABDV (1% mol.mol^{-1} of cross-linker) was added and the tube was then sealed. The polymerization was initiated by placing the tubes in an oil bath set at 45 °C. Polymerization was allowed to continue for a period of 24 hours, after which time the tubes were removed from the oil bath, broken with a hammer and the monolithic polymers removed. The resulting monoliths were lightly crushed to give smaller particles, which were extracted with a mixture of MeOH/AcOH (90/10, v/v) using a Soxhlet apparatus (60 mm x 94

mm) during 20 hours. The polymers were then crushed and sieved to 25-50 µm. These particles were subjected to sedimentation in acetone (4 times) to remove fine particles prior to further use. The washing extracts were evaporated to dryness and weighed. Non-imprinted polymers (NIPs) were prepared in the same manner as imprinted polymers (MIPs) for each formulation.

Imprinting efficiency evaluation by HPLC: Polymer particles (25–50 µm, 310 mg dry weight) were slurry packed into stainless steel HPLC columns (50 mm x 4.6 mm i.d.), using an SSI Pack-In-A-Box system (Restek, Paris, France) with MeOH/H_2O (4/1, v/v) mixture as the mobile phase at a continuous flow of 15 mL.min^{-1} for 4 min (~300 bars). The packed columns were then evaluated by HPLC injection method using an Agilent Infinity 1260 system equipped with a diode array detector and a binary pump (Agilent, Les Ulis, France). Acetonitrile with 1% acetic acid (v/v) was used as mobile phase for the organic phase behaviour and synthetic urine (**Table S2** and **S3**) for the aqueous phase behaviour and the column was equilibrated until a stable baseline was observed. For HPLC retention characterisation on the synthesized polymers, 5 mM stock solutions of nucleosides were prepared in deionised water, and diluted to 1mM, prior to analysis. HPLC analyses were performed by injecting 5 µL of 1mM analyte solutions at 25°C, using a flow rate of 1 mL.min^{-1}. The elution profiles were recorded at 260 nm. All injections were repeated several times (n=3), alternating between different analytes. The retention factors (k') of each analyte, were calculated as $k' = (t_R-t_0)/t_0$, where t_0 is the retention time of the void marker (acetone). Imprinting factors (IF) were calculated using the formula IF = k' (MIP)/k' (NIP). All these data are presented in **Table S2**, **Table S3,** and **Figure S3** and **Figure S4**.

Measurement of adsorption isotherms by HPLC frontal analysis: Staircase frontal chromatography was performed on each imprinted and non-imprinted polymer, with template TAcΨ. The mobile phase used was MeCN/AcOH (95/5, v/v) at 25 °C and at the flow rate of 1

$mL.min^{-1}$. A step-wise gradient was applied, mixing 10% increments of prepared template solutions in the mobile phase and pure mobile phase. Finally, a staircase frontal chromatogram with a total of 30 steps in the TAcΨ concentration range of 10^{-6} to 10^{-3} M was obtained. Therefore, the analysis was performed using three separate solutions of the corresponding template (10^{-6}-10^{-5}, 10^{-5}-10^{-4} and 10^{-4}-10^{-3} M), at the wavelength 260 or 280 nm depending on the saturation of the detector. The breakthrough volume for a non-retained analyte was measured by eluting the columns with MeCN/AcOH (95/5, v/v) containing 1% acetone (v/v %) as void marker. The obtained isotherms were fitted to Langmuir, Freundlich, Langmuir-Freundlich and Bi-Langmuir model, using the Origin Pro 8.5.1 software.

Modelling of frontal analysis: The raw data were adjusted to four mathematical models which account for the energetic heterogeneity of the polymers (Freundlich (FI), Langmuir (LI), Langmuir-Freundlich (L-FI) and Bi-Langmuir (Bi-LI)). The tested models use calculations based on isothermal (25 °C) equilibrium adsorption thermodynamics. From each concentration step, the corresponding amount of the bound analyte (Q) was calculated and plotted against the corresponding template concentration (Cf) in the mobile phase. The raw data were then fitted to theoretical isotherms using non-linear regression analysis (Table S7), and the affinity constants (K_a) and relative number of binding sites (N), and from some of the models the heterogeneity parameter (m), were obtained. The correlation coefficient (R^2) is one of the parameters frequently used as a measure of fit quality, although when the R^2 values of the fit are close between models (as obtained for MIP-2 and MIP-3), the Fisher value (F) can be used as a measure of choice of the best fit (**Figure 5** and **Table S5**).

BET measurements: Specific surface area (S_a), pore size (d_p) and pore volumes (V_p) as well as full nitrogen adsorption and desorption isotherms at 77K were analysed using Brunauer–Emmett–Teller (BET) model with ASAP 2020 surface area and porosity analyser

(Micromeritics Instrument Corporation, Creil, France). Polymers (100mg) were degassed overnight at 100°C, to remove adsorbed gases and moisture prior analysis (**Table S6**).

Solid phase extractions: Imprinted and non-imprinted particles (50 mg) were packed in 1 mL polypropylene cartridges between 20 μm porous polyethylene frits. The optimized MISPE protocol consisted of a cartridge conditioning step with 3 mL of MeOH, followed by 3 mL of deionized water, prior to loading 1 mL of synthetic urine[8] (**Figure S5** and **Table S7**) or real urine samples containing a mixture of Ψ with its analogues **5**, **6** and **7** (named Pseu mix) which could be find in the human urine (5 $\mu g.mL^{-1}$) (**Figure 6**). Following an initial aqueous WASH 1 (0.5 mL), 1 mL of organic solvent MeCN was used as WASH 2. Retained compounds were finally eluted with 3 mL of MeOH/formic acid (90/10, v/v). The extraction procedure was performed passing the sample and solutions through the cartridge by gravity, slowly pushing the liquid to maintain the 1 $mL.min^{-1}$ flow rate. For the real urine extraction, the morning urine samples were collected from 3 healthy volunteers (male and women) in the age between 23-30 years old, mixed together and kept at -20°C till one hour prior to analysis. The urine was of a normal smell, light yellow colour and pH 6-7. The collected synthetic and real urine extraction fractions were evaporated under a N_2 stream and re-solubilised in 0.5 mL of mobile phase A, and then analysed by HPLC-DAD (factor of concentration = 2).

HPLC method validation for pseudouridine detection in spiked urine samples: For the analysis of MISPE fractions, a linear gradient method with a mixture of mobile phase A (25 mM NH_4OAc buffer, pH=5.5) and B (MeCN/formic acid, 99.8/0.2, v/v) was developed. The gradient consisted of beginning on 10% B going to 15%B for 0-8 min (0.2 $mL.min^{-1}$), and then isocratic at 15%B for 8-30 min (0.3 $mL.min^{-1}$). The retention times were (time ± SD): 5-fluorouridine (**5**) (7 ± 0.08 min), pseudouridine (Ψ) (10 ± 0.1 min), uridine (**6**) (13 ± 0.1 min) and 5-methyluridine (**7**) (28 ± 0.05 min). The results of extraction were taken from the chromatographic analysis in a way that, for each nucleoside the peak area obtained after the

extraction step was divided by the one obtained before extraction (used as reference sample), giving finally the extraction % for that step. The calculated ratios were used to quantify the extraction performance for all MISPE steps (**Table S8**).

Supporting Information

Supporting Information is available from the Wiley Online Library or from the author.

Acknowledgements

This research was funded by French ANR-10-TECS-0004. AK is grateful to ANR for Ph.D. funding. Special thanks to Dr. B. Cagnon for BET analysis, Dr. M. Aumont-Nicaise for ITC analysis, M. D. Warszychi for DFT calculation, Dr. C. Lapthorn for HRMS. SL would like to thank the University of Kent for Ph.D. funding. Aleksandra Krstulja and Stefania Lettieri, contributed equally to this work.

References

[1] W. E. Cohn, J. Biol. Chem. 1960, **235**, 1488.

[2] S. Tamura, J. Fujii, T. Nakano, T. Hada, K. Higashino, Clin. Chim. Acta. 1986, **154**, 125.

[3] L.R. Solomon, T. R. Breitman, Biochem. Biophys. Res. Commun. 1971, **44**, 299.

[4] K. H. Schram, Mass Spectrometry Reviews. 1998, **17**, 131.

[5] K. Itoh, M. Mizugaki, N. Ishida, Clin. Chim. Acta. 1989, **181**, 305.

[6] M. D. Evans, D. Perrett, J. Lunce, K. E. Herbert, Ann. Clin. Biochem. 1997, **34**, 527.

[7] B. Kammerer, A. Frickenschmidt, C. H. Gleiter, S. Laufer, H. Liebich, J. Am. Soc. Mass Spectrom. 2005, **16**, 940.

[8] G. Mayes, M. J. Whitcombe, Adv. Drug Delivery Rev. 2005, **57**, 1742.

[9] L. Chen, S. Xua, J. Lia, Chem. Soc. Rev. 2011, **40**, 2922.

[10] C. Dejous, H. Hallil, V. Raimbault, J. L. Lachaud, B. Plano, R. Delépée, P. Favetta, L. Agrofoglio, D. Rebière, Sensors 2016, **16**, E915.

[11] L. Uzun, A. P. F. Turner, Biosens. Bioelectron. 2016, **76**, 131.

[12] G. Wulff, A. Sahran, Angew. Chem., Int. Ed. 1972, **11**, 341.

[13] K. Haupt, Nat. Mater. 2010, **9**, 612.

[14] K. Tanabe., T. Takeuchi, J. Matsui, K. Ikebukuro, K. Yano, I. Karube, I. Chem. Soc., Chem. Comm. 1995, 2303.

[15] R. J. Ansell. Adv Biochem Eng Biotechnol. 2015, **150**, 51.

[16] C. Lubke, M. Lubke, M. J. Whitcombe, E. N. Vulfson, Macromolecules 2000, **33**, 5098.

[17] A. J. Hall, P. Manesiotis, M. Emgenbroich, M. Quaglia, E. De Lorenzi, B. Sellergren, J. Org. Chem. 2005, **70**, 1732.

[18] A. Krstulja, S. Lettieri, A. J. Hall, R. Delépée, P. Favetta, L. A. Agrofoglio, Anal. Bioanal. Chem. 2014, **406**, 6275.

[19] D. A. Spivak, K. J. Shea, Macromolecules 1998, **31**, 2160.

[20] A. Krstulja, C. De Schutter, P. Favetta, P. Manesiotis, L. A. Agrofoglio, J. Chromatogr. A, 2014, **1365**, 12.

[21] K. Yano, K. Tanabe, T. Takeuchi, J. Matsui, J., K. Ikebukuro, I. Karube, Anal. Chim. Acta 1998, **363**, 111.

[22] P. Manesiotis, C. Borrelli, C. S. A. Aureliano, C. Svensson, B. Sellergren, J. Mater. Chem. 2009, **19**, 6185.

[23] A. Beltran, F. Borrull, P. A. G. Cormack, R. M. Marco, J. Chromatogr. A, 2011, **1218**, 4612.

[24] F. Herranz, M. D. S. María, R. M. Claramunt, Tetrahedron Lett. 2006, **47**, 9017.

[25] S. Chang, D. Van Engen, E. Fan, and A. D. Hamilton. J. Am. Chem. Soc., 1991, **113**, 7640.

[26] C. M. Hansen in Hansen Solubility Parameters: A User's Handbook, Second Edition, CRC Press, 2007, Ch. 17.

[27] W. L. Jorgensen, J. Pranata, J. Am. Chem. Soc. 1990, **112**, 2008.

[28] T. Uchimaru, J. Korchowiec, S. Tsuzuki, K. Matsumura, S. Kawahara, Chem. Phys. Lett. 2000, **318**, 203.

[29] C. Dethlefs, J. Eckelmann, H. Kobarg, T. Weyrich, S. Brammer, C. Näther, U. Lüning, Eur. J. Org. Chem. 2011, **2011**, 2066.

[30] B. T. Houseman, M. Mrksich, Topics in Current Chemistry, vol. 218 (Ed.: S. Penadès), Springer-Verlag, 2002, Ch. 1.

[31] M. Berger, F.P. Schmidtchen, J. Am. Chem. Soc. 1999, **121**, 9986.

[32] D. S. Janiak, P. Kofinas, Anal. Bioanal. Chem. 2007, **389**, 399.

[33] S. S. Madaeni, E. Salehi. Chem. Eng. J. 2009, **150**, 114.

[34] E. Rodríguez-Gonzalo, R. Hernández-Prieto, D. García-Gómez, R. Carabias-Martínez, J. Chromatogr.B. 2013, **942–943**, 21.

[35] W. E. Hull, R. E. Port, R. Herrmann, B. Britsch, W. Kunz, Cancer Res. 1988, **48**, 1680.

[36] G. Selvolini, G. Marrazza, Sensors 2017, **17**, 718.

[37] A. Winqvist, R. Strömberg, Eur. J. Org. Chem. 2008, **10**, 1705.

[38] K. Yano, K. Tanabe, T. Takeuchi, J. Matsui, J., K. Ikebukuro, I. Karube, Anal. Chim. Acta 1998, **363**, 111.

[39] J. Frank, Introduction to Computational Chemistry, second ed., John Wiley & Sons Inc., Chichester, England, 2007

[40] Jaguar, version 8.6, Schrödinger, LLC, New York, NY, 2014

[41] A. D. Bochevarov, E. Harder, T. F. Hughes, J. R. Greenwood, D. A. Braden, D. M. Philipp, D. Rinaldo, M. D. Halls, J. Zhang, R. A. Friesner, Int. J. Quantum Chem. 2013, **113**, 2110.

[42] J. Rebek, B. Askew, M. Killoran, D. Nemeth, F. T. Lin, J. Am. Chem. Soc. 1987, **109**, 2426.

[43] MicroCal, LLC, ITC Data Analysis in Origin®, Tutorial Guide Version 7.0, 2004

Figure 1. Structures of pseudouridine (Ψ) and uridine (U)

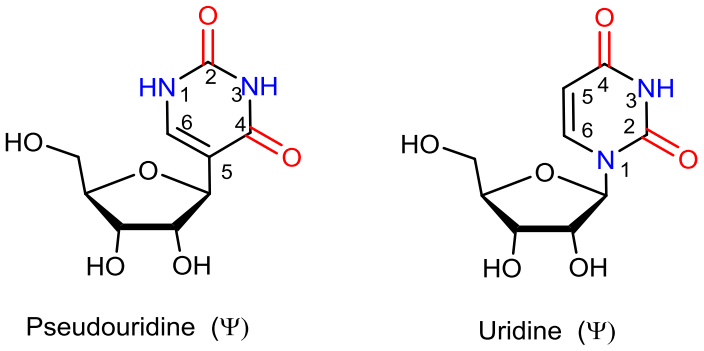

Figure 2. Template and monomers used for the development of polymer for Ψ recognition; Ψ, **TAc**Ψ, acrylamide (**1**), 2,6-bis(acrylamido)pyridine, (**2**), tailor-made monomer **3** and **4**.

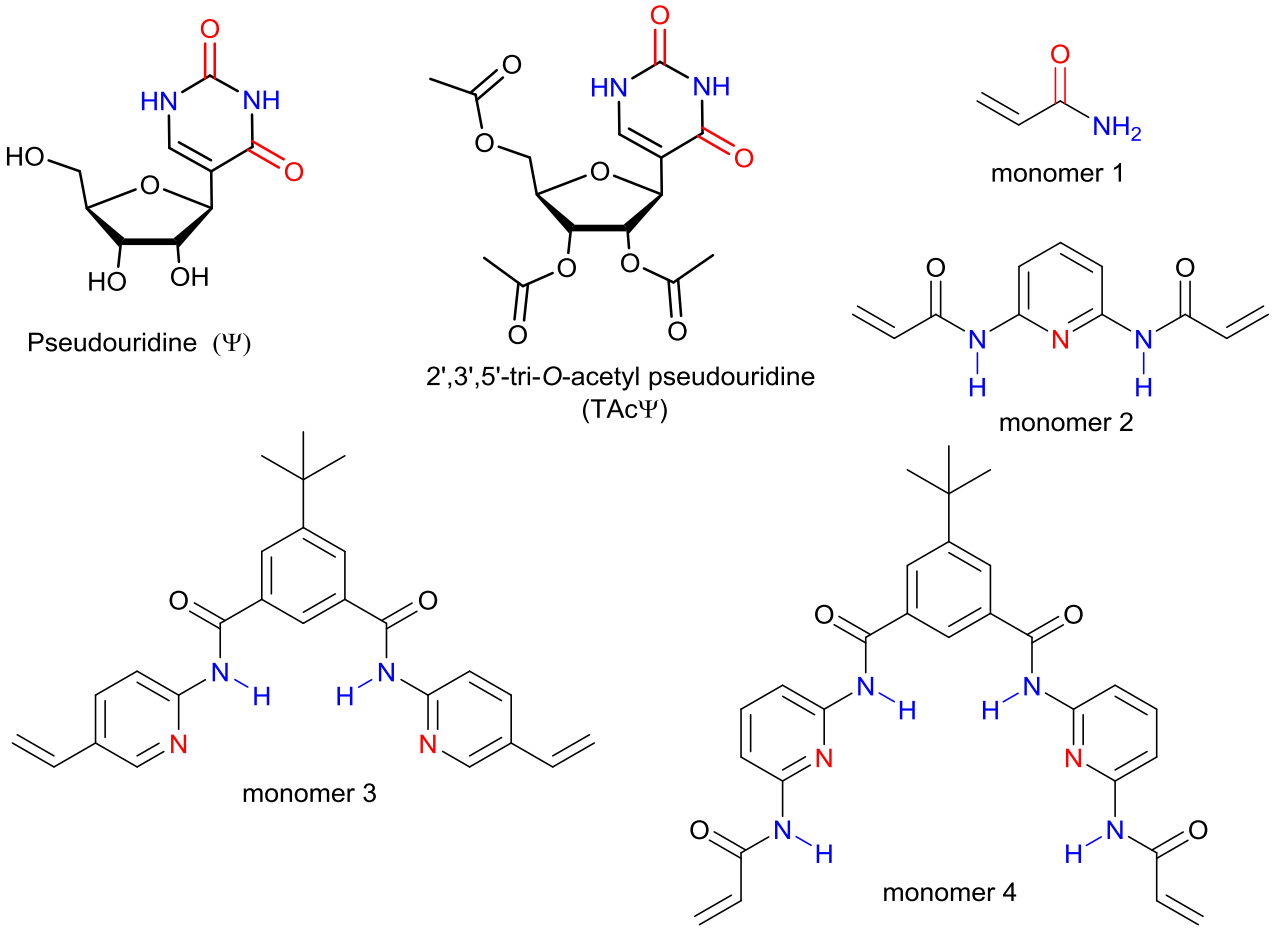

Figure 3. Theoretical presentation according to the ^{1}H-NMR results of template-monomer TAcΨ/**2** (A and D), TAcΨ/**3** (B and E) and TAcΨ/**4** (C and F) complexes with the possible hydrogen interactions (red dotted line), secondary negative interactions between the hydrogen bond donor groups (blue dotted line), and secondary negative interactions between the hydrogen bond acceptor groups (pink dotted line)

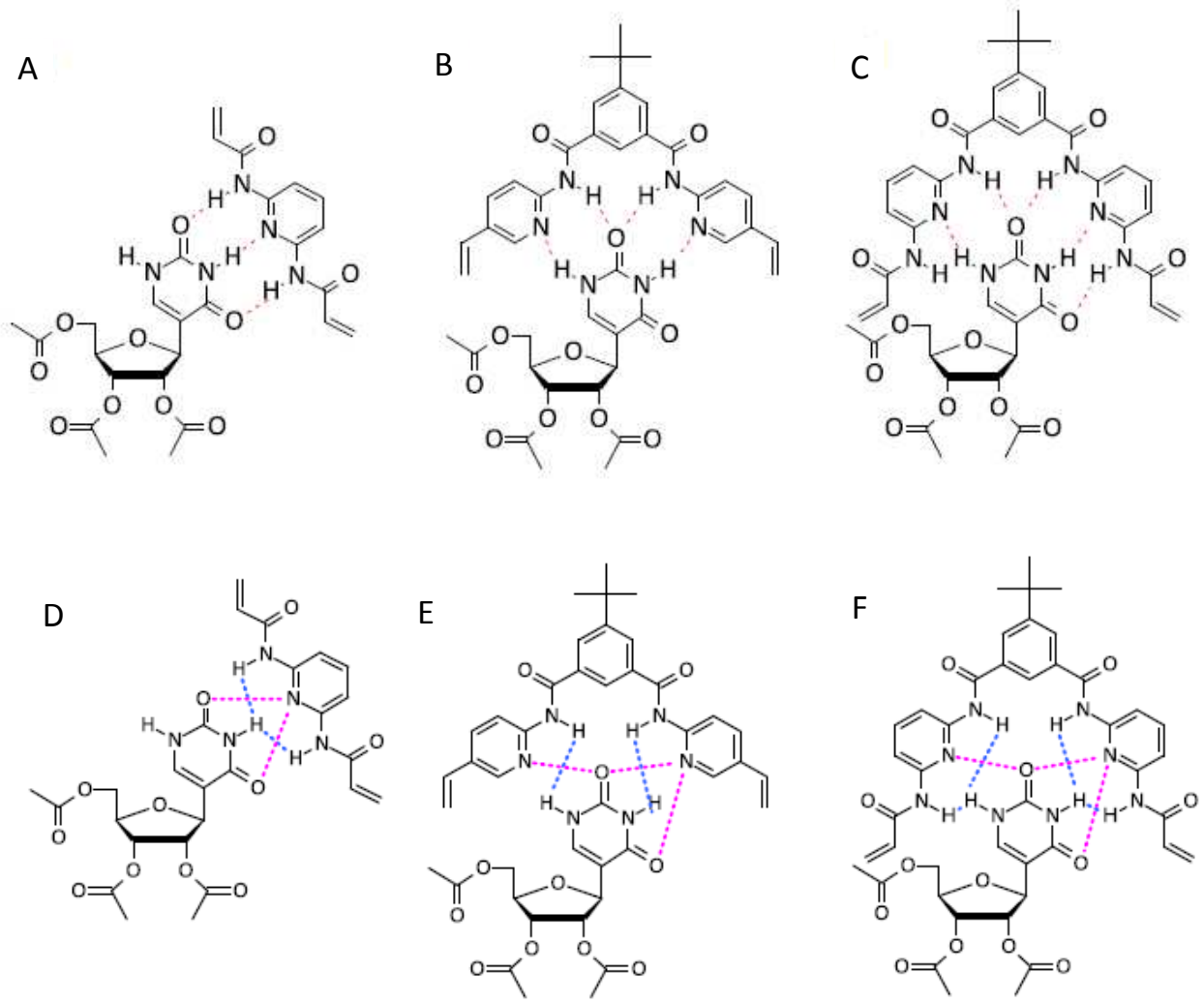

Figure 4. Urinary nucleosides and close pseudouridine (Ψ) analogues used for the HPLC evaluation of MIPs and NIPs (**1**, **2**, **3** and **4**)

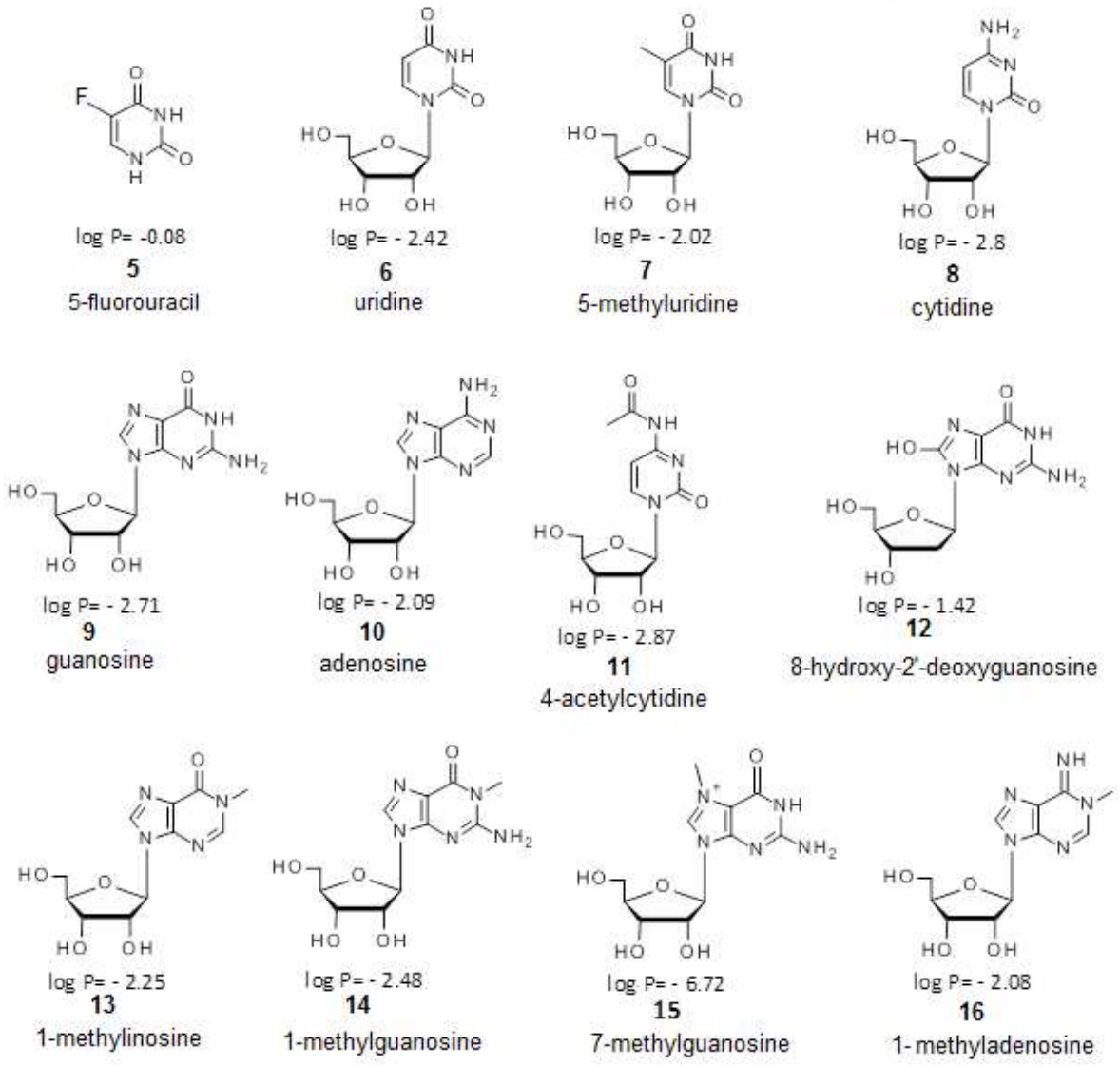

Figure 5. Experimental data obtained by frontal staircase method analysis for each MIP/NIP with the template analogue TAcΨ (MIP-1: cross, MIP-2: filled circles, MIP-3: filled diamonds and MIP-4: filled squares, NIP-1: cross, NIP-2: empty circles, NIP-3: empty

diamonds and NIP-4: empty squares). Inserted figure: data from the low concentration area, corresponding to theoretical high affinity sites (10^4 $M^{-1} \leq Ka \leq 10^6$ M^{-1}) for $K_{min} = 1/Cf_{min}$.

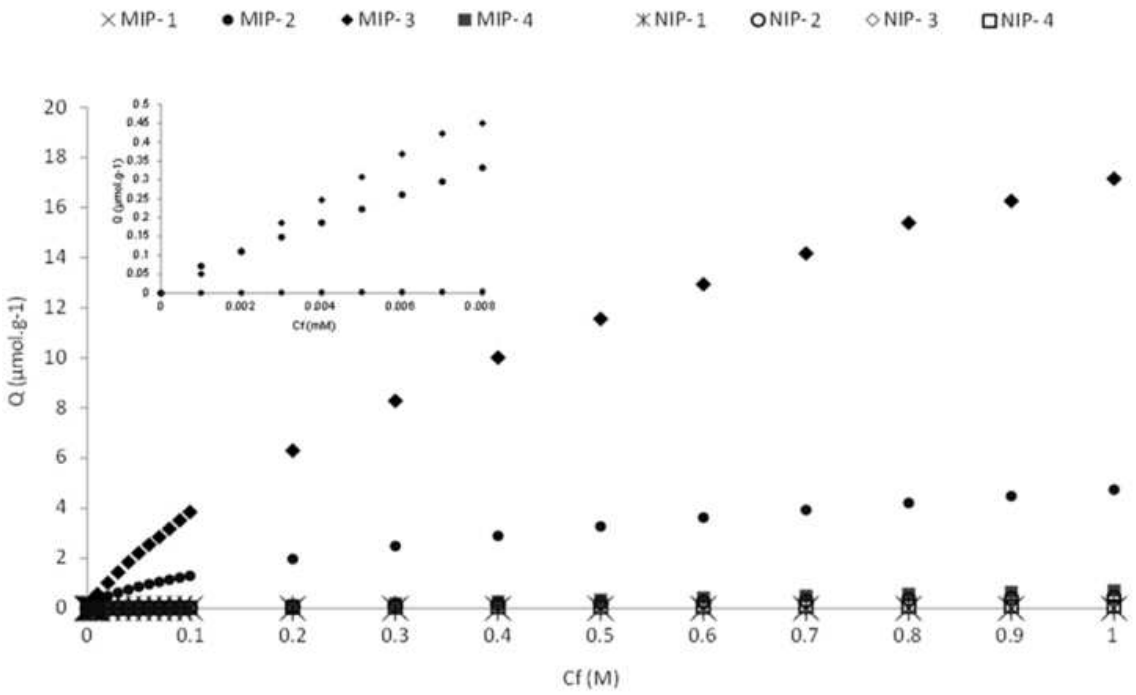

Figure 6. Chromatograms obtained during urine sample cleanup with MIP-3. HPLC analysis conditions: Hypercarb® (150x2.1 mm, 5µm) column, Mobile phase (A): NH_4OAc buffer (25 mM) pH 5.5, Mobile phase (B): MeCN/FA (99.8/0.2, v/v), gradient elution method used going from 10% B going to 15%B for 0-8 min (0.2 $mL.min^{-1}$), and then isocratic at 15%B for

8-30 min (0.3 mL.min^{-1}). Peak assignment: **5** (5-fluorouracil), Ψ (pseudouridine), **6** (uridine) and **7** (5-methyluridine). A: reference solution of Pseu mix (5 µg.mL^{-1}) in synthetic urine, B: non-spiked healthy urine, C: spiked healthy urine with Pseu mix (final concentration 5 µg.mL^{-1}), D: spiked urine recovery step on MIP-3 and E: spiked urine recovery step on NIP-3.

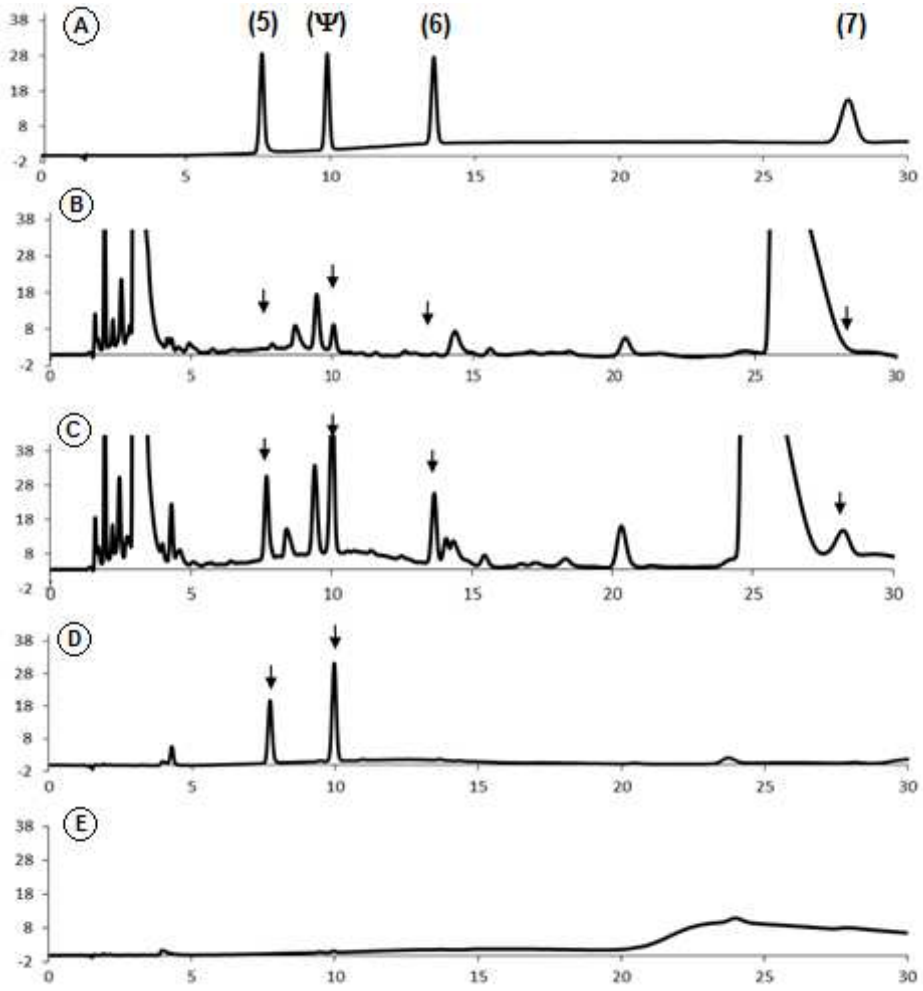

Table 1. Results of ^{1}H-NMR titration, ITC and DFT calculations to 1:1 binding model for pre-polymerization complexes; all data were calculated in chloroform, but also in mixture of solvent for DFT calculations with monomer **4**

Template/monomer complex	NMR titration		ITC measurement					DFT	
	K_{app} (M^{-1})	Δ_{HG} (ppm)	N	K_b (M^{-1})	ΔH	ΔS	ΔG	ΔG_{corr} (water)	ΔG_{corr} ($CHCl_3$)
TAcΨ/2	211 ± 3.62	2.27 ± 0.02	1.34 ± 0.02	1500±48	-2.9± 0.046	4.5	-4.2	-44.211	-49.027
TAcΨ/3	352 ± 49	0.80 ± 0.04	1 ± 0.02	379000±1450	-11.5± 0.059	-15	5.6	-51.255	-51.255
TAcΨ/4	117 ± 9.6	1.87 ± 0.09	/	/	/	/	/	/	/

Table 2. Formulations for imprinted and non-imprinted polymers.

POLYMER	TEMPLATE (mmol)	MONOMER (mmol)	EGDMA (mmol)	ABDV (g)	SOLVENT (mL)
MIP-1	TAcΨ (0.5)	**1** (1)	10	0.02	$CHCl_3$ (2.8)
MIP-2	TAcΨ (0.5)	**2** (0.5)	10	0.02	$CHCl_3$ (2.8)
MIP-3	TAcΨ (0.5)	**3** (0.5)	10	0.02	$CHCl_3$ (2.8)
MIP-4	TAcΨ (0.5)	**4** (0.5)	10	0.02	1,4-Dioxane / THF (1.5 / 0.5)
NIP-1	-	**1** (1)	10	0.02	$CHCl_3$ (2.8)
NIP-2	-	**2** (0.5)	10	0.02	$CHCl_3$ (2.8)
NIP-3	-	**3** (0.5)	10	0.02	$CHCl_3$ (2.8)
NIP-4	-	**4** (0.5)	10	0.02	1,4-Dioxane / THF (1.5 / 0.5)

Supporting Information

Tailor-made molecularly imprinted polymer for selective recognition of the urinary tumor marker pseudouridine

Aleksandra Krstulja Stefania Lettieri, Andrew J. Hall,* Vincent Roy, Patrick Favetta and Luigi A. Agrofoglio*

Content

Synthesis of 2',3',5'-tri-O-acetylpseudouridine (template, TAcΨ):

The synthesis was a modified version of previously reported procedure by Winqvist et al.[37] In short, pseudouridine (732 mg, 3 mmol) was stirred in dry pyridine (6 mL) and acetic anhydride (0.983 mL, 1.061 g, 10.5 mmol) at 20 °C under N_2 atmosphere for 25 hours. After this time, the reaction mixture was concentrated and the residue dissolved in dichloromethane (75 mL). The organic solution was washed with saturated aqueous $NaHCO_3$ (50 mL). The aqueous phase was then extracted with dichloromethane (4 x 50 mL) and the combined organic phases dried over $MgSO_4$. After filtration, the solvent was removed under vacuum to obtain a white solid, which was purified by chromatographic column (silica gel, 3% methanol in DCM). The TAcΨ template was obtained as a white solid and dried overnight under vacuum at 50°C to eliminate traces of pyridine and acetic acid. Finally, 930 mg of TAcΨ was obtained in 84% yield. ^{1}H-NMR (400 MHz, $CDCl_3$): δ 2.08, 2.10 and 2.11 (s, 9H, C(O)CH_3), 4.25-4.30 (m, ^{3}J=5.2 Hz, 2H, H5'), 4.358-4.40 (m, ^{3}J=4.8 Hz, 1H, H4'), 4.89 (d, ^{3}J=4.4 Hz, 1H, H1'), 5.27 (t, ^{3}J=5.6 Hz, 1H, H3'), 5.37 (t, ^{3}J=5.2 Hz, 1 H, H2'), 7.54 (s, 1 H, H6), 9.97 (s, 2H, NH). ^{13}C-NMR (100 MHz, $CDCl_3$): δ 20.5, 20.7 and 20.9 (C(O)CH_3), 63.6 (C-5'), 71.2 (C-3'), 74.0 (C-2'), 77.5 (C-1'), 78.4 (C-4'), 111.4, 139.3 (C-6), 152.4, 162.8, 169.8, 169.9, 171.1. IR: 1131.7, 1227.0, 1508.4, 1579.1, 1675.2, 1723.2, 2962.6, 3225.7 cm^{-1}. HRMS (ESI) m/z: $[M+H]^+$ calcd for $C_{15}H_{19}N_2O_9$, 371.109; found, 371.108.

Synthesis of 2,6-bis(acrylamido)pyridine (monomer 2):

The synthesis was based on previously reported procedure by K. Yano et al.[38] To a solution of 2,6-diaminopyridine (**8**, 2 g, 0.018 mol), triethylamine (0.055 mol, 7.66 mL) and anhydrous dichloromethane (150 mL), 3.72 mL of acryloyl chloride (0.0458 mol) dissolved in 15 mL of dichloromethane was added slowly in an ice bath and under a dinitrogen atmosphere. The reaction mixture was stirred at room temperature overnight. The next day water was added to

quench any unreacted acryloyl chloride. The organic layer was then extracted with saturated aqueous sodium bicarbonate (2 x 100 mL) and brine (100 mL). The organic layer was collected and dried over $MgSO_4$, filtered and distilled. The residue was then purified by column chromatography (6:4, petroleum ether-ethyl acetate). The monomer was precipitated into petrol ether from dichloromethane to obtain monomer **2** as white crystals (1.73g, 45%). ^{1}H NMR (100 MHz, DMSO-d_6): δ 5.79 (dd, ^{2}J=2 Hz, ^{3}J=10.2 Hz, 2H, -CH_{cis} =), 6.31 (dd, ^{2}J=2 Hz, ^{3}J=17 Hz, 2H, -CH_{trans}=), 6.65 (dd, $^3J_{cis}$=10 Hz, $^3J_{trans}$=17.2 Hz , 2H, CH=), 7.79 (dd, ^{3}J=6.8, 2.4 Hz, 1H, CH-Ar), 7.87 (d, ^{3}J=7.2 Hz, 2H, CH-Ar), 10.31 (s, 2H, NH) ppm. ^{13}C NMR (100 MHz, $CDCl_3$): δ 110.2 (CH-Ar), 128.8 (CH_2=), 130.8 (CH=), 141.0 (C-H), 149.5 (C=O), 163.5 (C=N) ppm. IR: 694.7, 979, 1313, 1584, 1677, 3325 cm^{-1}. M.p. = 115-118°C. HRMS (ESI-TOF) m/z: $[M+H]^+$ calcd for $C_{11}H_{11}N_3O_2H$, 218.22; found, 218.0934.

Synthesis of 1,3-bis[[5-vinylpyrid-2-yl)amido]carbonyl]5-tert-butyl-benzene (monomer 3):

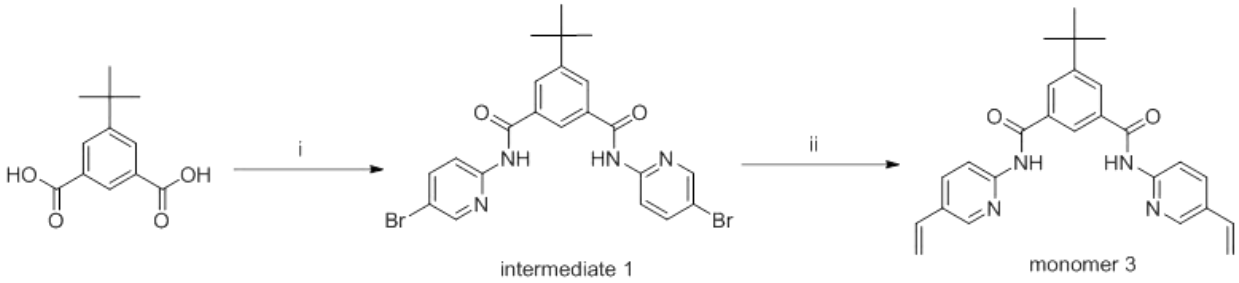

(i) 5-Tert-butyl isophthalic acid (27.9 mmol, 6.2 g) and 2-amino-5-bromopyridine (63 mmol, 10.73 g) were dissolved in 16.7 mL of dimethylformamide. Pyridine (15.74 mL, 82mmol) was added and the mixture left to react for 30 minutes. Then, T3P (50 wt% in DMF, 94.32 mmol, 60 mL) was added dropwise at -20 ºC (ice-NaCl bath) after which the reaction was left to stir overnight at room temperature. The next day the solvent was removed and the crude product precipitated in water and filtered. The brown solid was sonicated for 30 minutes in 100mL 1 N aqueous NaOH (twice) and filtered. The white solid was dried overnight to obtain 5.2 g of **intermediate 1** (35%). ^{1}H NMR (400 MHz, DMSO-d_6): δ 1.38 (s, 9H, tert-butyl-

CH_3), 8.11 (dd, ^2J=2.4 Hz, ^3J=9.2 Hz, 2H, -CH^4), 8.20 (d, ^3J=1.6 Hz, 2H, -CH_3), 8.24 (d, ^3J=8.8 Hz, 2H, -CH^6), 8.44 (t, ^3J=1.6 Hz, 1H, Ph-CH-2), 8.55 (dd, ^2J= 0.8 Hz, ^3J=2.4 Hz, 2H, Ph-CH-4 and 6), 11.10 (s, 2H, NH). ^{13}C NMR (100 MHz, DMSO-d_6): δ 31.4 (tert-butyl-CH_3), 35.4 (tert-butyl-C), 114.6 (Py-CH_2[C-5]), 116.6 and 141.3 (Py-CH_2[C-3] & Py-CH_2[C-4]), 125.7 (Ph-C-2), 129.0 (Ph-C-4), 134.2, 149.1 (Py-CH_2[C-6]), 151.7, 152.1, 166.2. HRMS (ESI-TOF) m/z: [M-H^+] calcd for $C_{22}H_{20}Br_2N_4O_2$, 532.23; found, 531.0032. IR: 740, 881. 1091, 1213, 1369, 1499, 1566, 1683, 2962, 3423 cm^{-1}. M.p. = 227-228°C

(ii) A stirred solution of **intermediate 1** (2.9 g, 5.45 mmol) in DME under dinitrogen atmosphere was treated with palladium(0)tetrakis-triphenylphosphine (0.552 mmol, 0.638 g). The reaction mixture was stirred at room temperature for 20 minutes and 2,4,6-trivinylcyclotriboroxane (5.64 mmol, 1.36 g), K_2CO_3 (11.28 mmol, 1.56 g) and water were added. The reaction mixture was heated under reflux (108 °C) for 2 hours. The reaction mixture was concentrated and the crude product precipitated from water. The crude product was purified by column chromatography (dry column: alumina, PE:EtOAc 7:3) to obtain **monomer 3** (1.13 g, 49%). ^{1}H NMR (400 MHz, DMSO-d_6): δ 1.39 (s, 9H, tert-butyl-CH_3), 5.34 (dd, ^2J=2 Hz, ^3J=11.2Hz, 2H, CH_{cis} =), 5.93 (dd, ^3J=18 Hz, 2H, CH_{trans}=), 6.77 (dd, $^3J_{cis}$=11.2 Hz, $^3J_{trans}$= 17.6 Hz, 2H, -CH=), 8.06 (dd, ^2J=2.4 Hz, ^3J=8.8 Hz, 2H, -CH^4), 8.20 (d, ^3J=1.2 Hz, 2H, -CH^3), 8.28 (d, ^3J=8.8 Hz, 2H, -CH^6), 8.46 (s, 1H, Ph-CH-2), 8.49 (d, ^3J=2.4 Hz, 2H, Ph-CH-4 and 6), 10.99 (s, 2H, NH). ^{13}C NMR (100 MHz, DMSO-d_6): δ 31.4 (tert-butyl-CH_3), 35.4 (tert-butyl-C), 114.6 (-CH=), 115.6 (CH_2=), 125.5 (Ph-C-2), 128.9 (Ph-C-4 and 6), 129.6, 133.5 (Py-CH_2[C-4]), 134.4 (Py-CH_2[C-3]), 146.9 (Py-CH_2[C-6]), 135.4, 152.0, 152.2, 166.1. HRMS (ESI-TOF) m/z: [M+$H]^+$ calcd for $C_{26}H_{26}N_4O_2H$, 427.51; found, 427.2128. IR: 905.2, 1633.3, 1676.7, 2962.1, 3089.1, 3239.3 cm^{-1}. M.p. = 152-161°C.

Synthesis of 1,3-bis[[6-bisacrylamid-2-yl)amido]carbonyl]5-tert-butyl-benzene (monomer 4)

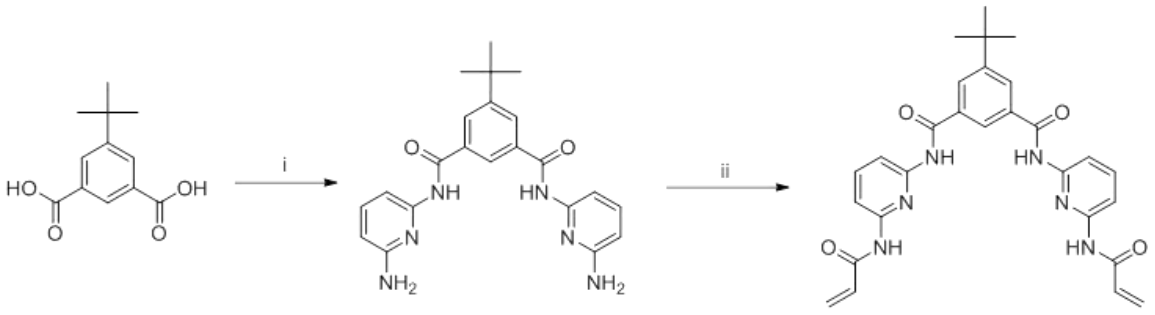

(i)

(i) 1,3-bis[[6-amino-2-yl)amido]carbonyl]5-tert-butyl-benzene (intermediate 2). 5-tert-butilisophthalic acid (3 g, 0.0135 mol, 1eq) was refluxed with 20 mL of $SOCl_2$ for 4 h. The solvent was then evaporated to obtain the corresponding diacid chloride, which was dissolved in 20 mL of dry THF and added dropwise to a solution of 2,6-diaminopyridine (14.73 g, 0.135 mol, 10 eq) and triethylamine (TEA) (3.76 mL, 2.73 g, 0.027 mol, d=0.726) in anhydrous THF (220 mL) at 0°C and under dinitrogen atmosphere. The reaction mixture was stirred at room temperature overnight. The next day the solvent was evaporated and the crude product washed with water. The sticky solid was filtered, dissolved in hot ethyl acetate and filtered again. The filtrate was evaporated to obtain a brown solid, which was then purified with a chromatographic column using silica gel as the stationary phase and ethyl acetate as the eluent. The first fraction coming out of the column was the desired intermediate (light brown solid, 88%). ^{1}H NMR (400 MHz, DMSO-d_6): δ 1.37 (s, 9H, tert-butyl-CH_3), 5.79 (s, 4H, NH_2), 6.29 (dd, ^{2}J=0.8 Hz, ^{3}J=8 Hz, 2H, Py-CH_2[H-5]), 7.41 (dd, ^{2}J=0.8 Hz, ^{3}J=8 Hz, 2H, Py-CH_2[H-3]), 7.45 (t, ^{3}J=7.6 Hz, 2H, Py-CH_2[H-4]), 8.11 (d, ^{3}J=1.2 Hz, 2H, Ph-CH-4 and 6), 8.33 (s, 1H, Ph-CH-2), 10.292 (s, 2H, NH). ^{13}C NMR (100 MHz, DMSO-d_6): δ 31.5 (tert-butyl-CH_3), 35.3 (tert-butyl-C), 102.4 (Py-CH_2[C-5]), 104.6 and 139.5 (Py-CH_2[C-3 and C-4]), 124.8 (Ph-C-2), 128.5 (Ph-C-4 and 6), 134.6, 150.9, 151.9, 159.1, and 165.7. HRMS (ESI-TOF) m/z: $[M+H]^+$ calcd for $C_{22}H_{25}N_6O_2H$, 405.46; found, 405.203. IR: 1526.6, 1614.9, 1697.4, 2965.1, 3317.4, 3450.2 cm^{-1}. M.p.: 99-104 ºC.

(ii) 1,3-bis[[6-bisacrylamid-2-yl)amido]carbonyl]5-tert-butyl-benzene (monomer **4**). To a solution of **intermediate 2** (3.5g, 8.65 mmol, 1 eq) and triethylamine (3.61 mL, 2.62 g, 25.95 mmol, d=0.726, 3 eq) in anhydrous THF (180 mL), 1.75 mL of acryloyl chloride (1.95 g, 21.62 mmol, FW=90.51, d=1.114, 2.5 eq) in 20 mL of THF was added slowly at 0°C and under dinitrogen atmosphere. The reaction mixture was stirred at room temperature overnight. The next day the precipitate was filtered off and the solvent evaporated. The residue was washed with water and a saturated solution of sodium bicarbonate ($NaHCO_3$). The solid was then sonicated in 100 mL of DCM. Monomer 1 was obtained as a white solid in a 52% yield (2.3g). ^{1}H NMR (400 MHz, DMSO-d_6): δ 1.41 (s, 9H, tert-butyl-CH_3), 5.80 (dd, ^{2}J=2 Hz, ^{3}J=12 Hz, 2H, CH_{cis} =), 6.33 (dd, ^{2}J=1.6 Hz, ^{3}J=20 Hz, 2H, CH_{trans}=), 6.67 (dd, $^3J_{cis}$=10.4 Hz, $^3J_{trans}$=16. Hz, 2H, -CH=), 7.87 (m, ^{3}J=8 Hz, 4H, Py-CH_2[H-3 and H-4]), 7.95 (m, ^{3}J=4 Hz, 2H, Py-CH_2[H-5]), 8.21 (d, ^{3}J=1.6 Hz, 2H, Ph-CH-4 and 6), 8.382 (s, 1H, Ph-CH-2), 10.45 (s, 2H, NH-C^6), 10.59 (s, 2H, NH-C^2). ^{13}C NMR (100 MHz, DMSO-d_6): δ 31.5 (tert-butyl-CH_3), 35.5 (tert-butyl-C), 110.7 (Py-CH_2[C-5]), 111.5 and 140.7 (Py-CH_2[C-3 and C-4]), 125.7 (Ph-C-2), 128.4 (CH_2=), 128.6 (Ph-C-4 and 6), 132.1 (-CH=), 134.6, 150.9, 151.0, 152.0, 164.3 and 166.1. HRMS (ESI-TOF) m/z: $[M+H]^+$ calcd for $C_{28}H_{29}N_6O_4H$, 513.56; found, 513.224. IR: 977.6, 1638.9, 1691.6, 2962, 3277.5 cm^{-1}. M. p.: 223-229 ºC.

Table S1. The solubility results of TAcΨ and monomers (**1-4**).

Solvent	T° (°C)	δP[a]	δH[b]	Dielectric constant	Monomer Solubility (mM)	Template Solubility (mM)
Chloroform	25	3.1	5.7	4.81	≤ 100 (**1**) ≤ 100 (**2**) ≤ 100 (**3**) ≤ 100 (**4**)	≤ 100
Acetonitrile	25	18	6.1	37.5	≤ 100 (**1**) ≤ 100 (**2**) ≤ 100 (**3**) ≤ 100 (**4**)	≤ 100
Dimethyl sulfoxide	25	16.4	10.2	46.68	≤ 300 mM (**1**) ≤ 300 mM (**2**) ≤ 300 mM (**3**) ≤ 50 mM (**4**)	≤ 500
1,4-dioxane/THF (3/1, v/v)	25	2.77	4.25	3.59	N.D. (**1**) N.D. (**2**) N.D. (**3**) ≤ 100 mM (**4**)	≤ 100 mM

Hansen solubility parameters ($MPa^{1/2}$): [a] polarity [b] hydrogen bonding ability ; N.D. : not determined

Figure S1.A: ^{1}H-NMR titration of monomer **2** with 2',3',5'-Tri-O-acetylpseudouridine

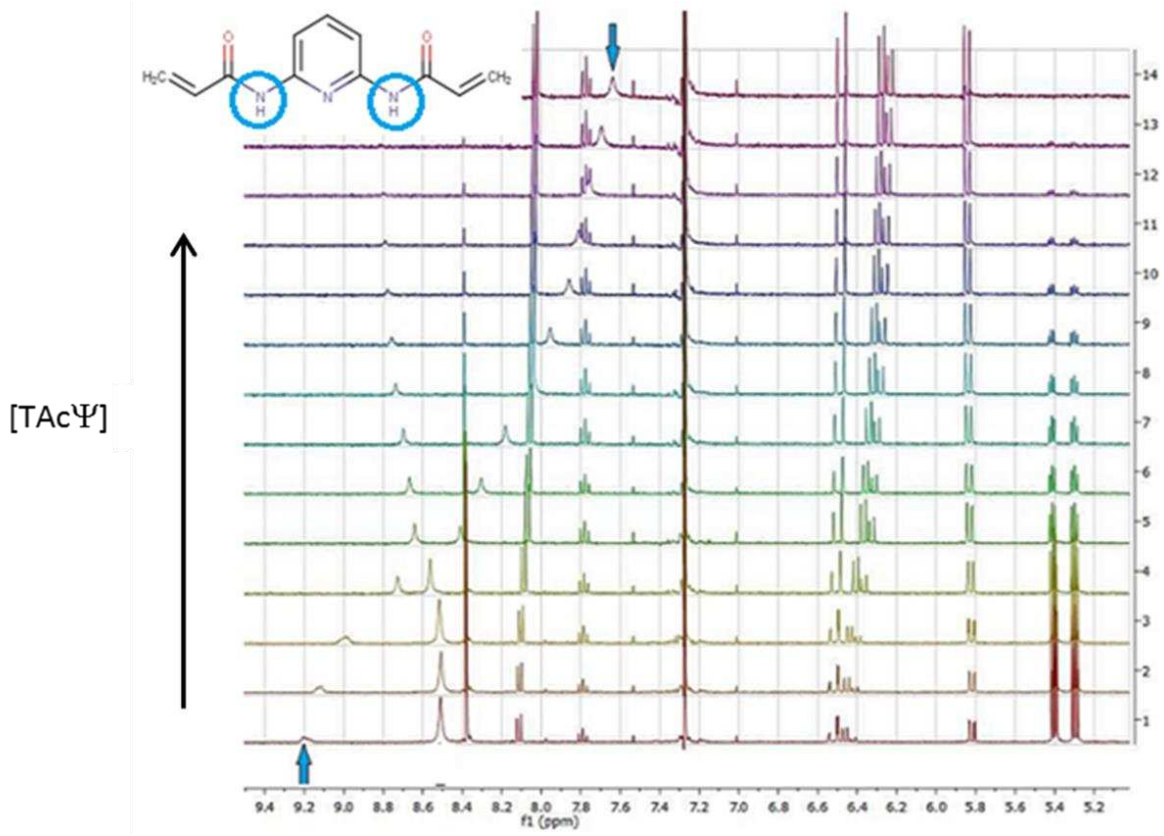

Figure S1.B: ^{1}H-NMR titration of monomer **3** with 2',3',5'-Tri-O-acetylpseudouridine

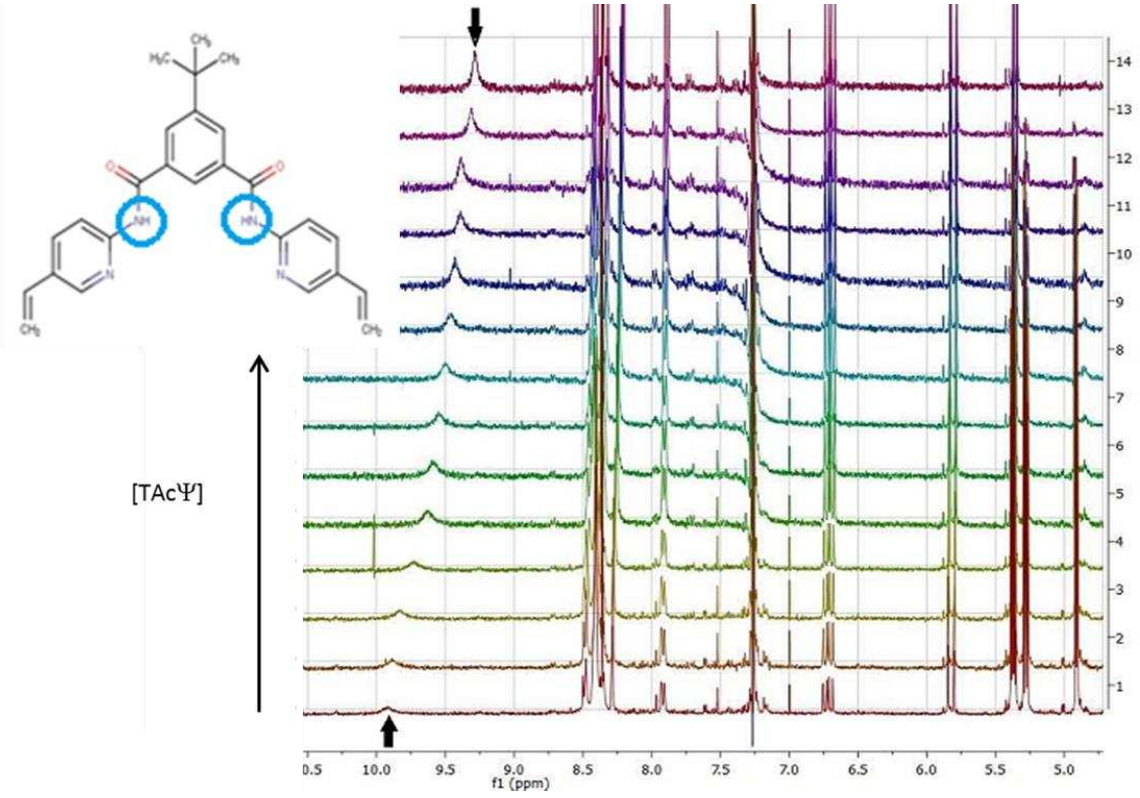

Figure S1.C: ^{1}H-NMR titration of monomer **4** with 2',3',5'-Tri-O-acetylpseudouridine

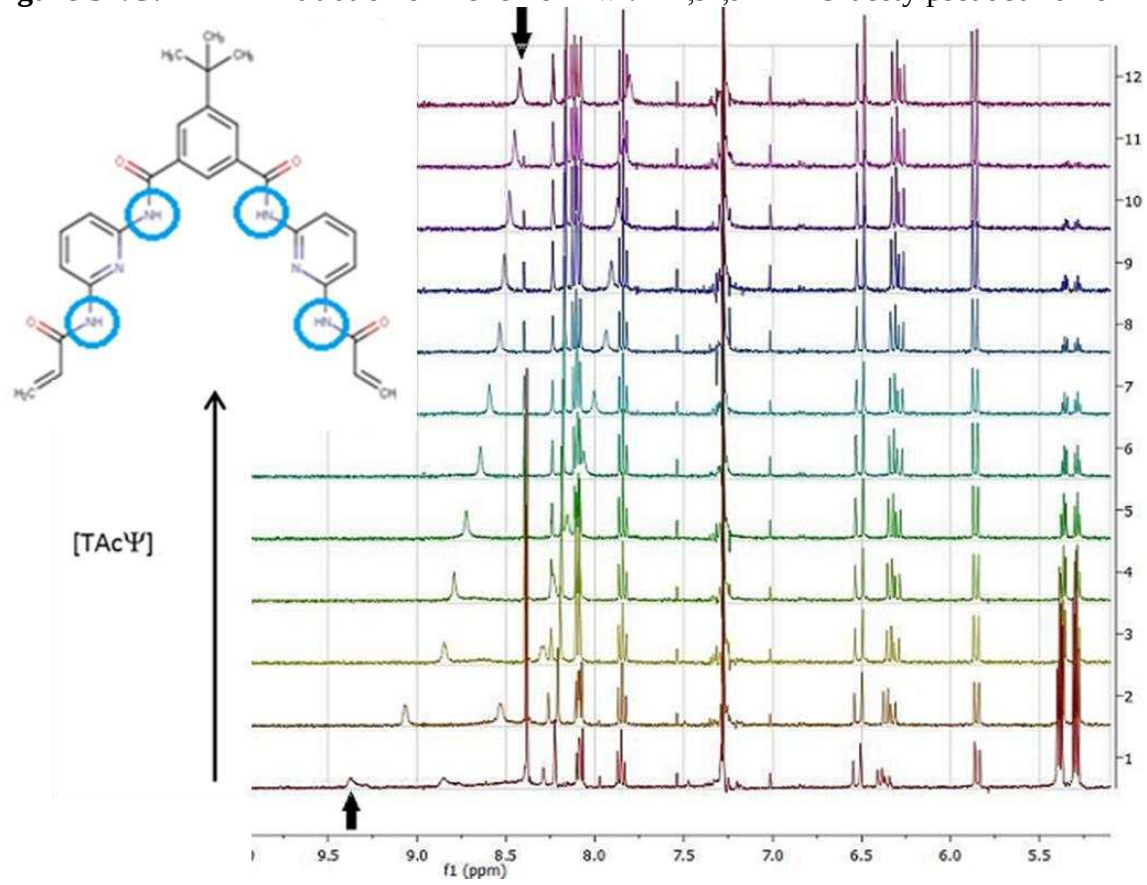

Figure S2. ITC measurement results for A) TAcΨ **/2** and B) TAcΨ **/3** complexations

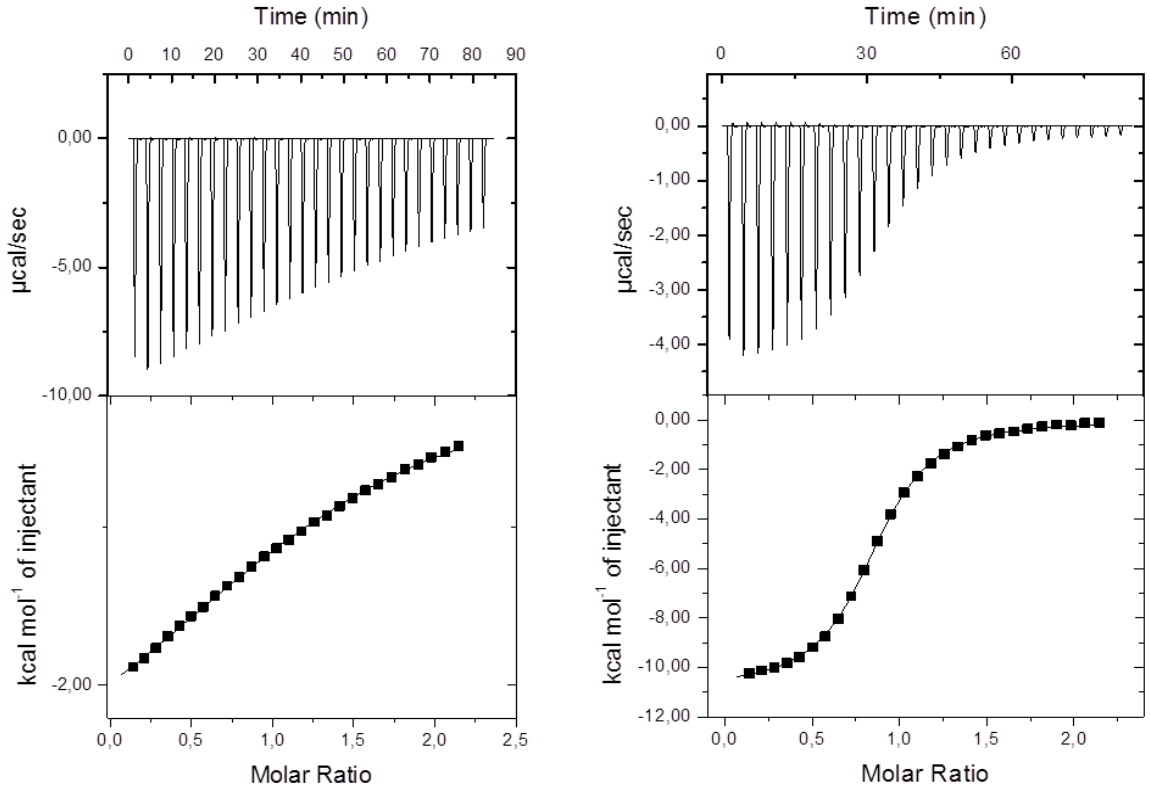

Table S2. HPLC polymer retention analysis of MIP-1, MIP-2, MIP-3 and MIP-4, and corresponding NIPs, in organic mobile phase

MeCN /AcOH (99 /1, v/v)															
Polymer	**Parameter**	**TAc Ψ**	**Ψ**	**6**	**7**	**8**	**9**	**10**	**11**	**12**	**13**	**14**	**15**	**16**	**RSD [d] %**
MIP–1	k ± SD[c]		4.25±0.05	1.52±0.2	1.32±0.05	2.47±0.04	4.82±0.3	3.11±0.2	1.71±0.04	9.29±0.74	4.93±0.05	1.02±0.02	3.43±0.03	2.17±0.04	< 10
	α(Ψ)	0.23	1.00	2.79	3.22	1.72	0.88	1.37	2.48	0.46	0.86	4.17	1.24	1.96	
	IF	18.45	1.62	1.13	1.20	0.86	1.03	1.81	1.35	1.21	7.25	0.94	1.27	2.24	
MIP–2	k ± SD	>40*	>40*	32.78±0.5	16.99±0.8	8.45±0.7	2.17±0.04	1.3±0.03	1.23±0.06	11.69±0.8	6.02±0.05	1±0.08	2.49±0.12	1.62±0.06	< 5
	α(Ψ)	N/D	N/D	N/D	N/D	N/D	N/D	N/D	N/D	N/D	N/D	N/D	N/D	N/D	
	IF	>91	>29	20.11	10.11	4.97	4.43	1.57	0.89	1.94	13.09	2.22	1.98	3.24	
MIP–3	k ± SD	>40*	>40*	>40*	13.91±0.7	9.31±0.07	7.55±0.25	5.07±0.03	5.62±0.06	10.05±0.2	4.95±0.25	1.7±0.3	6.19±0.04	4.58±0.01	< 5
	α(Ψ)	N/D	N/D	N/D	N/D	N/D	N/D	N/D	N/D	N/D	N/D	N/D	N/D	N/D	
	IF	>65	>25	>2	1.06	5.48	5.07	4.49	9.06	1.05	8.25	2.46	5.20	6.03	
MIP–4	k ± SD	21.09±0.08	19.79±0.3	16.05±0.5	13.12±0.4	4.18±0.2	5.14±0.8	6.83±0.5	5.71±0.3	10.61±0.3	3.53±0.4	1.2±0.05	2.36±0.06	2.14±0.04	< 5
	α(Ψ)	0.94	1.00	1.23	1.51	4.73	3.85	2.90	3.46	1.87	5.61	16.49	8.39	9.25	
	IF	19.53	2.92	3.77	3.12	3.34	2.04	3.25	4.57	1.23	12.17	2.67	2.59	1.26	
NIP–1	k ± SD	0.99±0.05	2.62±0.03	1.35±0.04	1.1±0.02	2.88±0.07	4.68±0.08	1.72±0.5	1.27±0.4	7.7±0.52	0.68±0.04	1.09±0.06	2.7±0.8	0.97±0.09	< 6
	α(Ψ)	2.65	1.00	1.94	2.38	0.91	0.56	1.52	2.06	0.34	3.85	2.40	0.97	2.70	
NIP–2	k ± SD	0.44±0.2	1.36±0.05	1.63±0.25	1.68±0.5	1.7±07	0.49±0.8	0.83±0.6	1.38±0.04	6.03±0.06	0.46±0.5	0.45±0.5	1.26±0.9	0.5±0.04	< 6
	α(Ψ)	3.09	1.00	0.83	0.81	0.80	2.77	1.64	0.99	0.23	2.96	3.02	1.08	2.72	
NIP–3	k ± SD	0.62±0.08	1.62±0.09	17.32±0.5	13.18±0.4	1.7±0.2	1.49±0.06	1.13±0.4	0.62±0.8	9.58±0.07	0.6±0.09	0.69±0.04	1.19±0.6	0.76±0.03	< 6
	α(Ψ)	2.61	1.00	0.09	0.12	0.95	1.09	1.43	2.61	0.17	2.70	2.35	1.36	2.13	
NIP–4	k ± SD	1.08±0.01	6.78±0.5	4.26±0.03	4.21±0.04	1.25±0.06	2.52±0.09	2.10±0.04	1.25±0.05	8.63±0.2	0.29±0.07	0.45±0.08	0.91±0.09	1.70±0.6	< 8
	α(Ψ)	6.28	1.00	1.59	1.61	5.42	2.69	3.23	5.42	0.79	23.38	15.07	7.45	3.99	

[a] α (Ψ) = k_t(Ψ)/ k_x; pseudouridine (Ψ) , x = structurally related analyte
k = (t_R-t_0)/t_0; t_0 = retention time of acetone (0.75±-0.01) , t_R = retention time of analyte,
[b] IF = k (MIP)/k (NIP).
[C] SD (standard deviation of analysis, n=3)
* Elution time > 40 min, N/D (non-determinate)
[d] RSD % = (SD/mean)* 100

Table S3. HPLC polymer retention analysis of MIP-1, MIP-2, MIP-3 and MIP-4, and corresponding NIPs, in aqueous mobile phase

Synthetic urine															
Polymer	**Parameter**	**TAc Ψ**	**Ψ**	**6**	**7**	**8**	**9**	**10**	**11**	**12**	**13**	**14**	**15**	**16**	**RSD [d] %**
MIP–1	k ± SD[c]	0.6±0.05	0.11±0.6	0.15±0.09	1.67±0.8	0.22±0.06	2.09±0.06	5.83±0.07	2.94±0.06	6.17±0.02	1.78±0.06	3.67±0.09	3.81±0.02	13.22±0.4	< 8
	α(Ψ)	0.18	1.00	0.73	0.07	0.50	0.05	0.02	0.04	0.02	0.06	0.03	0.03	0.01	
	IF	1.87	0.42	0.20	0.95	0.81	0.96	0.86	0.93	0.91	1.01	1.00	1.44	1.13	
MIP–2	k ± SD	36.2±0.06	2.65±0.5	1.94±0.1	3.07±0.2	0.1±0.05	1.22±0.03	7.33±0.2	3.79±0.05	7.46±0.09	2.5±0.3	4.49±0.5	0.21±0.06	1.18±0.2	< 6
	α(Ψ)	0.07	1.00	1.37	0.86	26.50	2.17	0.36	0.70	0.36	1.06	0.59	12.62	2.25	
	IF	2.36	44.17	3.18	1.00	0.50	0.74	1.09	1.20	1.18	1.64	0.82	0.48	0.14	
MIP–3	k ± SD	36.3±0.08	17±0.06	2.7±0.03	3.39±0.4	0.42±0.03	2.75±0.06	10.96±0.1	5.52±0.07	13.6±0.06	2.19±0.04	7.99±0.6	0.47±0.03	12.1±0.06	< 5
	α(Ψ)	0.47	1.00	6.30	5.01	40.48	6.18	1.55	3.08	1.25	7.76	2.13	36.17	1.40	
	IF	8.58	70.83	3.80	1.57	4.20	1.42	1.51	1.53	1.98	1.53	1.27	4.27	1.26	
MIP–4	k ± SD	6.35±0.03	0.94±0.06	1.85±0.5	4.29±0.1	0.51±0.3	5.04±0.4	4.35±0.02	6.82±0.3	14.9±0.4	3.88±0.6	6.88±0.2	1±0.06	24.2±0.2	< 10
	α(Ψ)	0.15	1.00	0.51	0.22	1.84	0.19	0.22	0.14	0.06	0.24	0.14	0.94	0.04	
	IF	1.41	3.03	2.08	1.87	1.24	1.77	0.49	1.78	1.70	1.87	1.90	3.45	1.27	
NIP–1	k ± SD	0.32±0.02	0.26±0.09	0.75±0.5	1.75±0.08	0.27±0.04	2.18±0.06	6.8±0.1	3.17±0.5	6.81±0.5	1.76±0.08	3.66±0.04	2.65±0.03	11.71±0.3	< 6
	α(Ψ)	0.81	1.00	0.35	0.15	0.96	0.12	0.04	0.08	0.04	0.15	0.07	0.10	0.02	
NIP–2	k ± SD	15.36±0.5	0.06±0.04	0.61±0.02	3.08±0.3	0.2±0.05	1.64±0.6	6.73±0.02	3.16±0.08	6.32±0.05	1.52±0.2	5.5±0.7	0.44±0.03	8.36±0.9	< 8
	α(Ψ)	0.00	1.00	0.10	0.02	0.30	0.04	0.01	0.02	0.01	0.04	0.01	0.14	0.01	
NIP–3	k ± SD	4.23±0.03	0.24±0.06	0.71±0.3	2.16±0.8	0.1±0.02	1.94±0.4	7.24±0.04	3.6±0.09	6.88±0.4	1.43±0.06	6.31±0.02	0.11±0.03	9.58±0.04	< 6
	α(Ψ)	0.06	1.00	0.34	0.11	2.40	0.12	0.03	0.07	0.03	0.17	0.04	2.18	0.02	
NIP–4	k ± SD	4.49±0.6	0.31±0.05	0.89±0.01	2.29±0.6	0.41±0.3	2.84±0.09	8.91±0.06	3.83±0.3	8.76±0.05	2.07±0.08	3.64±0.05	0.29±0.04	19±0.7	< 10
	α(Ψ)	0.07	1.00	0.35	0.14	0.76	0.11	0.03	0.08	0.04	0.15	0.09	1.07	0.02	

[a] α (Ψ) = k_t/ k_x; pseudouridine (Ψ) , x = structurally related analyte
k = (t_R-t_0)/t_0; t_0 = retention time of acetone (0.95±-0.01) , t_R = retention time of analyte,
[b] IF = k (MIP)/k (NIP).
[C] SD (standard deviation of analysis, n=3)
* Elution time > 40 min, N/D (non-determinate)

Figure S3. Retention factors (k) and imprinting factor (IF) for target Ψ and its analogues injected in organic mobile phase on MIP-1, MIP-2, MIP-3 and MIP-4 (A and C) and on NIP -1, NIP-2, NIP-3 and NIP-4 (B**)** polymer packed columns. HPLC conditions: MeCN-AcOH (99/1, v/v) as mobile phase, 1mL.min^{-1} flow rate, 5µL injection volume of 1 mM nucleoside solution, $t_{(run)}$= 40 min, UV detection at 260 nm.

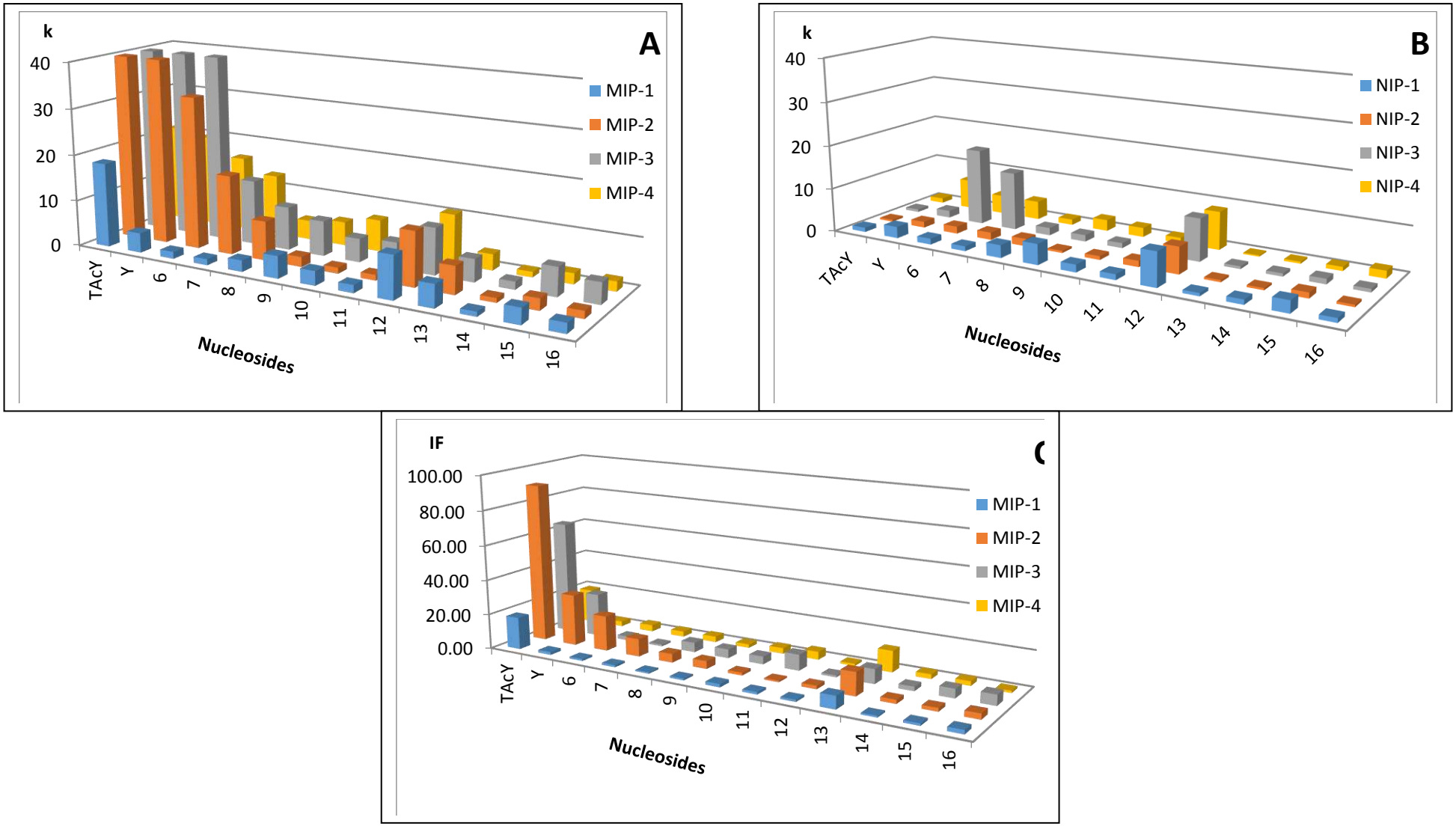

Figure S4. Figure 3. Retention factors (k) and imprinting factor (IF) for target Ψ and its analogues injected in synthetic urine as mobile phase on MIP -1 to MIP-4 (A) and on NIP-1 to NIP-4 (B) polymer packed columns. IF value are presented on graph C. HPLC conditions: synthetic urine as mobile phase, 1mL.min^{-1} flow rate, 5µL injection volume of 1 mM nucleoside solution, t(run)= 40 min, UV detection at 260 nm.

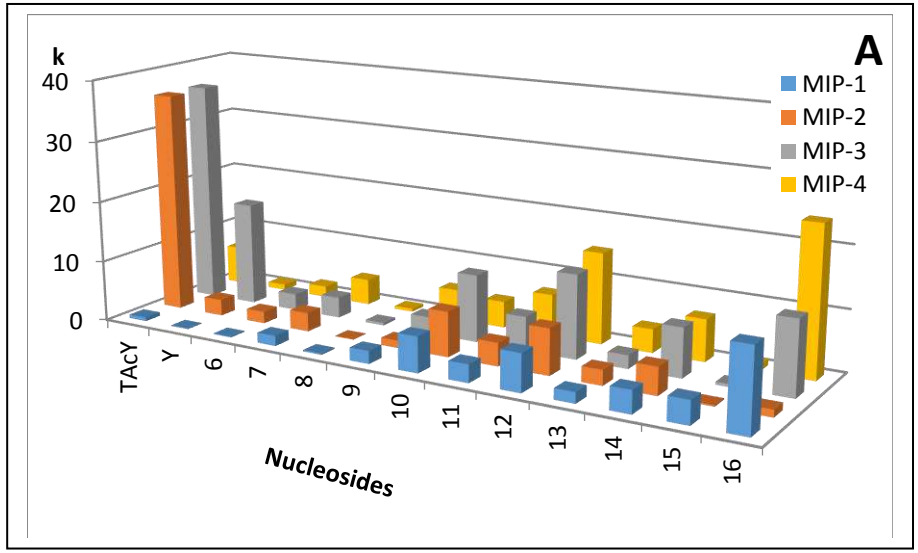

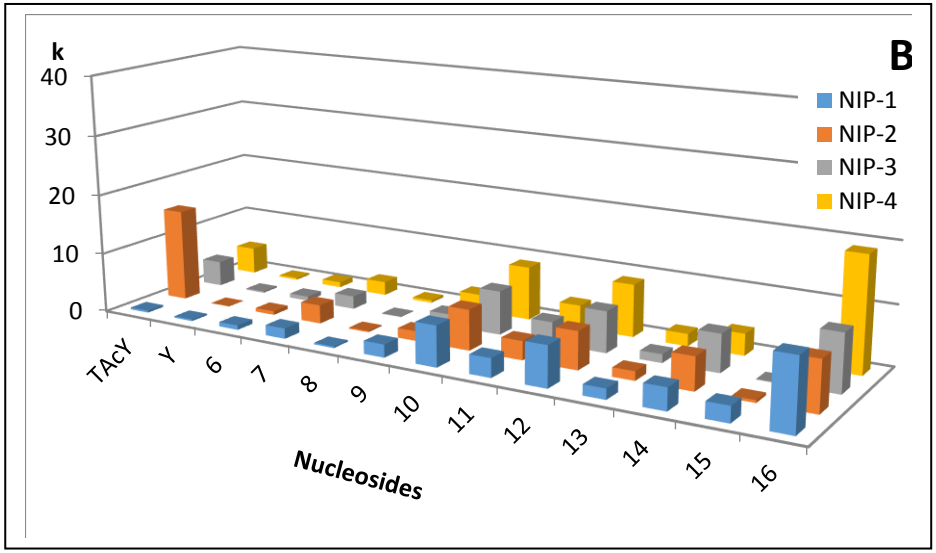

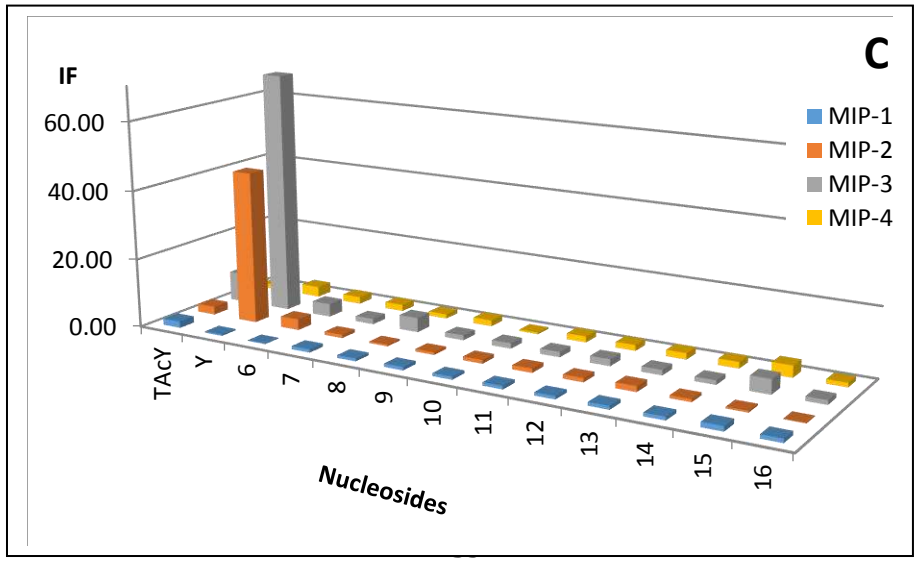

Table S4. Composition of synthetic urine used.[1]

Compound	Mass (g)[a]	Final concentration (mM)
Urea	2.425	200
Uric acid	0.034	1
Creatinine	0.085	4
$Na_3C_6H_5O_7$	0.299	5
NaCl	0.632	54
KCl	0.451	30
NH_4Cl	0.162	15
$CaCl_2$	0.09	3
$MgSO_4$	0.1	2
$NaHCO_3$	0.04	2
$Na_2C_2O_4$	0.007	0.1
Na_2SO_4	0.256	9
NaH_2PO_4	0.1	3.6
Na_2HPO_4	0.011	0.4

Table S5. Frontal chromatography results for MIPs and NIPs (1, 2, 3 and 4); affinity constants (K_a, $L.mol^{-1}$), number of binding sites (N, $\mu mol.g^{-1}$), sum of least squares (R^2) and the Fisher test value (F) are presented.

MIP																			
Binding model	**MIP-1**					**MIP-2**					**MIP-3**					**MIP-4**			
	K_a	N	m	R^2	F test	K_a	N	m	R^2	F test	K_a	N	m	R^2	F test	K_a	N	m	R^2	F test
Langmuir			N.D.[c]			$0.3x10^3$	6.27	-	0.9883	2300	$1x10^3$	29	-	0.997	11800	$9.9x10^3$	3.83	-	0.9986	13300
Bi-Langmuir			N.D.[c]			$0.8x10^3$ $0.49x10^3$	0.02 3.8	-	0.9999	75010	$9.5x10^3$ $0.63x10^3$	3.78 43.63	-	0.9997	422000			N.D.[c]		
Freundlich[a]	$0.46x10^3$	0.93	0.67	0.9996	61080	$53x10^3$	1.54	0.56	0.9996	45080	$16x10^3$	10.05	0.63	0.9985	16750	$9.4x10^3$	1.42	0.73	0.9965	6600
Langmuir-Freundlich[b]	$0.26x10^3$	4.18	1	0.999	23800	$0.04x10^3$	34	0.6	0.9999	26300	$40.8x10^3$	53	0.8	0.9998	199000	$0.64x10^3$	4.87	0.92	0.9988	16200
NIP																				
Binding model	**NIP-1**					**NIP-2**					**NIP-3**					**NIP-4**				
	K_a	N	m	R^2	F test	K_a	N	m	R^2	F test	K_a	N	m	R^2	F test	K_a	N	m	R^2	F test
Langmuir	$1.9x10^3$	0.12	-	0.995	7800			N.D.[c]					N.D.[c]			$0.2x10^3$	3.57	-	0.997	6800
Bi-Langmuir			N.D.[c]					N.D.[c]					N.D.[c]					N.D.[c]		
Freundlich[a]	$29x10^3$	0.04	0.62	0.996	5200	$3x10^3$	1.06	0.95	0.9998	151000	$0.4x10^3$	1.06	0.95	0.9998	18000	$1x10^3$	0.58	0.92	0.9955	4700
Langmuir-Freundlich[b]	$0.49x10^3$	0.23	0.76	0.998	9600	$0.1x10^3$	4.99	1.12	0.9999	290000			N.D.[c]			$0.86x10^3$	0.2	1	0.9981	7300

[a] Average Ka and N values calculated from Rushton *et al*.[2]

[b] Average Ka calculated using $Ka= a^{1/m}$

[C] N/D, fit did not converge

Table S6. Specific surface areas (Sa), mean pore diameters (dp) and pore volume (Vp) measured by BET for **MIP-** and **NIP- 1**, **2**, **3** and **4**

Polymer	BET S_a [$m^2.g^{-1}$]	d_P [Å]	V_P [$cm^3.g^{-1}$]
MIP-1	218	71	0.25
NIP-1	210	72	0.22
MIP-2	146	68	0.10
NIP-2	141	118	0.07
MIP-3	296	72	0.302
NIP-3	9	350	0.003
MIP-4	204	67	0.25
NIP-4	196	63	0.19

S_a- Surface area, d_P- Pore diameter, V_P- Pore volume

Figure S5. Recoveries of uridine (**6**), 5-methyluridine (**7**), 5-fluorouracil (**5**) and pseudouridine (Ψ) from synthetic urine after each step of the optimized MISPE protocol, on A) MIP-3 and B) NIP-3 (error bars representing SD were calculated with n=3).

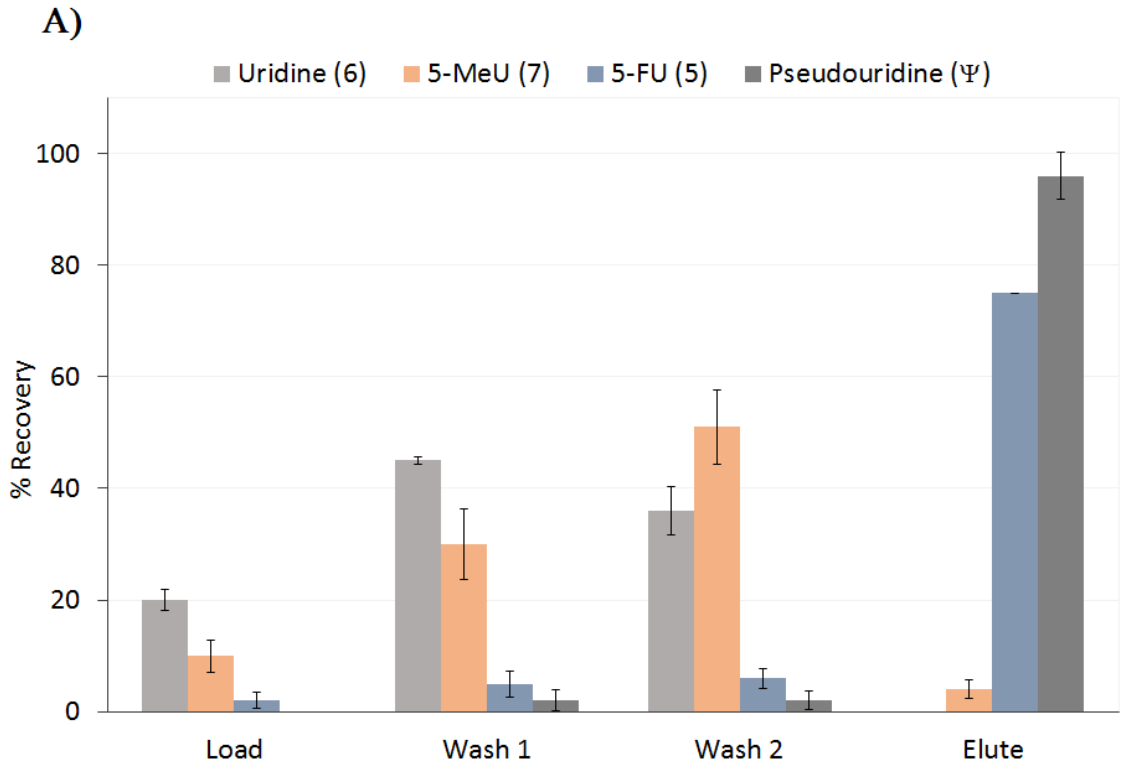

B)

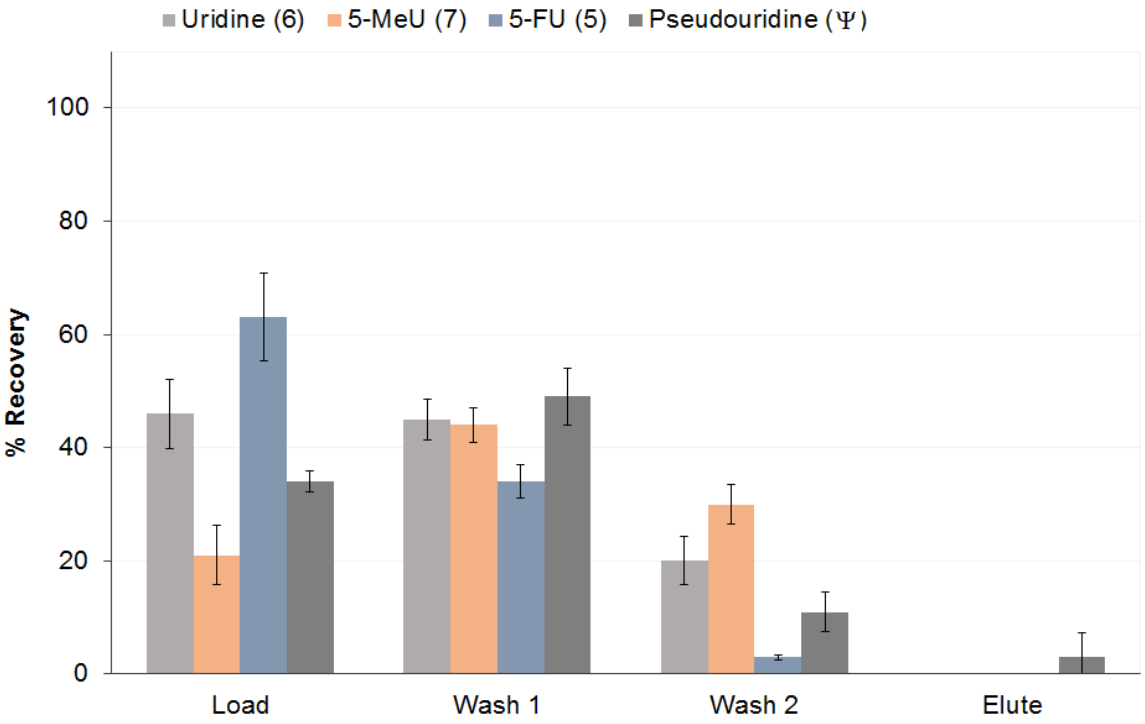

Table S7. Nucleoside recoveries (%) from real urine samples (n=3) on MIP-3/NIP-3 with calculated statistical parameters.[3]

Nucleoside	Mean%±SD[a] MIP-3	Mean% ±SD NIP-3	$RSD_{(MIP)}$[b]
5	41 ± 8	2 ± 1	19
Ψ	92 ± 2	2 ± 2	7
6	2 ± 2	1 ± 0.5	13
7	5 ± 1	1 ± 1	16

[a] Standard deviation (SD) = $\Sigma(Xi\text{-}\bar{X})^2/n\text{-}1$
[b] Relative standard deviation (RSD)= $(SD/\bar{X})*100$

Table S8. Linearity of detector response for the HPLC analysis.[3]

	Nucleoside analyte			
	5	**Ψ**	**6**	**7**
Linear regression				
R^2	0.9997	0.9999	0.9991	0.9999
Slope	44.31	48.95	55.65	34.23
y-intercept	-48.52	5.94	18.63	35.16
Calculated detector response tests (α=5%)				
Cochran (C_{th} (6;2) = 0.62)	0.59	0.55	0.56	0.56
Fisher ($F1_{th}$(1;16) = 4.49)	78.3x 10^3	164.2x 10^3	18.2x 10^3	169.3x 103
Fisher ($F2_{th}$(4;12) = 5.91)	0.62	1.76	0.08	2.44
Repeatabilities (ANOVA test)				
LOQ (µg.mL^{-1})	3.81	4.26	4.64	4.8
LOD (µg.mL^{-1})	1.27	1.77	1.39	1.63
[a] t_R (min)	7.68	10.08	14.5	28.14
[b] F	0.41	0.49	3.08	1.91
P-value	0.62	0.67	0.09	0.2

[a] retention time mean value , [b] Fcrit= 4.26

[1] S. Chutipongtanate, V. Thongboonkerd, Anal. Biochem. **2010**, 402, 110.

[2] G.T. Rushton, C.L. Karns, K. D. Shimizu., Anal. Chim. Acta **2005**, 528, 107.

[3] Z. B. Alfassi, Z. Boger, Y. Ronen, in Statistical Treatment of Analytical Data, Blackwell Publishing Ltd., **2009**, Ch.1.

The table of contents

The development of technologies able to recognize selectively tumor biomarker is vital to help its prognosis and diagnosis. That's why, for the first time, a selective tailor-made imprinted polymer material to the marker pseudouridine, is synthetized. Here we demonstrate the MIP selectivity and efficiency in human urine and open doors to its use in disposable sensors.

Keywords: pseudouridine, tailor-made monomer, molecular recognition, imprinted polymer, cancer

Aleksandra Krstulja Stefania Lettieri, Andrew J. Hall,* Patrick Favetta, Vincent Roy, and Luigi A. Agrofoglio*

Tailor-made molecularly imprinted polymer for selective recognition of the urinary tumor marker pseudouridine

TOC Figure: